Published in final edited form as:

J Immunol. 2019 June 01; 202(11): 3267–3281. doi:10.4049/jimmunol.1801466.

Tissue Inhibitor of Metalloproteinase-1 (TIMP-1) Promotes PMN Pericellular Proteolysis by Anchoring Matrix Metalloproteinase-8 and -9 to PMN Surfaces

Xiaoyun Wang, PhD[†], **Joselyn Rojas-Quintero, MD, MSc**[†], **Julie Wilder, PhD**[‖], **Yohannes Tesfaigzi, PhD**[‖], **Duo Zhang, PhD**[§], **Caroline A. Owen, MD, PhD**[1,†,*]

[†]The Division of Pulmonary and Critical Care Medicine, Brigham & Women's Hospital and Harvard Medical School, Boston, MA, 02115, USA;

[‖]The Lovelace Respiratory Research Institute, Albuquerque, NM, 87108, USA;

[§]Pulmonary Center, Boston University School of Medicine, Boston, MA, 02118, USA.

Abstract

Matrix metalloproteinase (MMP)-8 and -9 released by degranulating PMNs promote pericellular proteolysis by binding to PMN surfaces in catalytically-active, but tissue inhibitor of metalloproteinases (TIMP)-resistant forms. The PMN receptor(s) to which MMP-8 and MMP-9 bind(s) is not known. Competitive binding experiments showed that Mmp-8 and Mmp-9 share binding sites on murine PMN surfaces. A novel form of TIMP-1 (an inhibitor of soluble MMPs) is rapidly expressed on PMNs surfaces when human PMNs are activated. Membrane-bound TIMP-1 is the PMN receptor for pro and active MMP-8 and -9 as: 1) TIMP-1 is strikingly co-localized with MMP-8 and -9 on activated human PMN surfaces and in PMN extracellular traps; 2) minimal immunoreactive and active Mmp-8 or Mmp-9 are detected on the surface of activated *Timp-1*$^{-/-}$ murine PMNs; 3) binding of exogenous Timp-1 (but not Timp-2) to *Timp-1*$^{-/-}$ murine PMNs reconstitutes the binding of exogenous proMmp-8 and proMmp-9 to the surface of *Timp-1*$^{-/-}$ PMNs. Unlike full length proMmp-8 and proMmp-9, mutant proMmp proteins lacking the COOH-terminal hemopexin domain fail to bind to *Mmp-8*$^{-/-}$*xMmp-9*$^{-/-}$ murine PMNs. Soluble hemopexin inhibits the binding of proMmp-8 and proMmp-9 to *Mmp-8*$^{-/-}$*xMmp-9*$^{-/-}$ murine PMNs. Thus, the COOH-terminal hemopexin domains of proMmp-8 and proMmp-9 are required for their binding to membrane-bound Timp-1 on murine PMNs. Exposing non-human primates to cigarette smoke upregulates co-localized expression of TIMP-1 with MMP-8 and MMP-9 on

[1]This work was supported by Public Health Service, National Heart, Lung, and Blood Institute Grants HL063137, HL086814, HL111835, and AI111475–01, Flight Attendants Medical Research Institute grants #CIA123046 and The Department of Defense (CDMRP) grant # PR152060.

[*]Address for correspondence: Caroline A. Owen, MD, PhD; Division of Pulmonary and Critical Care Medicine, Brigham and Women's Hospital, 60 Fenwood Road, 3rd Floor, Room 3016H, Boston, MA 02115. Phone: 617-525-5408; Fax: 617-525-5413; cowen@bwh.harvard.edu.

Author Contributions: CO conceived the project and designed the experiments; XW, JR, JW, YT, DZ, and CO conducted experiments and contributed to data analysis and interpretation. All authors contributed to the writing and editing of the manuscript.

Conflict of Interest: Caroline Owen is an employee of Vertex Pharmaceuticals Inc., but has no conflicts of interest relevant to the focus of this manuscript. The other authors declare that they have no conflicts of interest with the contents of this article.

[3]Some of the results reported in this manuscript have been published previously in the form of an abstract that was presented at a conference (69).

peripheral blood PMN surfaces. By anchoring MMP-8 and MMP-9 to PMN surfaces, membrane-bound TIMP-1 plays a counterintuitive role in promoting PMN pericellular proteolysis occurring in COPD and other diseases.

Keywords

Receptor; inflammation; pericellular proteolysis; cigarette smoke; COPD; non-human primate; neutrophil extracellular trap

INTRODUCTION

Matrix metalloproteinase-1 (MMP-8[2]; neutrophil collagenase) and MMP-9 (gelatinase B) are members of the MMP subfamily of zinc-dependent metalloproteinases. MMP-9 is ubiquitously expressed by leukocytes and structural cells in most organs in humans and mice. MMP-8 is highly expressed by human and murine PMNs (1,2), but is also expressed at lower levels by activated macrophages, vascular smooth muscle cells, and bronchial epithelial cells in humans and mice (3,4).

MMP-9 cleaves a wide variety of extracellular matrix (ECM) proteins (5) and various non-matrix proteins to alter their biologic activities (6–13). Mmp-9 promotes the development of aneurysms in mice by degrading ECM proteins present in vessel walls (14), but also promotes small airway fibrosis developing in animals exposed chronically to cigarette smoke (CS) or allergens by increasing ECM deposition (15,16). Mmp-9 increases the accumulation of inflammatory cells in the airways of mice with allergic airway inflammation (17–19) and regulates the severity of acute lung injury in mice (20,21).

MMP-8 is an interstitial collagen-degrading proteinase *in vitro*. Murine Mmp-8 has crucial activities in regulating inflammatory responses to injury in various organs by cleaving chemokines (2,22,23). Mmp-8 also participates in a proteolytic cascade (along with Mmp-9 and a serine proteinase) in the generation of Pro-Gly-Pro tripeptide fragments of collagen which promote PMN influx into the lungs of mice (24).

MMP-8 and MMP-9 both contribute to human PMN-mediated proteolysis (2,25,26), but do not regulate murine PMN migration (2,27). Neither proteinase is synthesized *de novo* by mature PMNs. MMP-8 and -9 are produced in PMN precursors in the bone marrow, and then stored within the specific and gelatinase granules of PMNs, respectively (28). When PMNs are activated, proMMP-8 and -9 are released from PMNs into the extracellular space. Extracellular MMP-8 and -9 are activated by the cysteine switch mechanism, and their activities are restrained by the four members of the tissue inhibitor of metalloproteinase (TIMP) family (29).

MMP-8 and -9 are also expressed as membrane-associated proteinases on the surface of human and murine PMNs when activated *in vitro* (25,26,30,31). Activation of PMN with degranulating agonists results in rapid translocation of both MMPs from PMN granules to the plasma membrane. Membrane-bound MMP-8 and MMP-9 have similar catalytic activities and efficiencies as the soluble forms of these MMPs, but differ from the soluble

MMP forms by their resistance to inhibition by TIMPs (25,26). Membrane-bound forms of pro and active forms of MMP-8 have been detected on circulating PMNs in human subjects with a chronic lung disease (32). Membrane-bound Mmp-8 is the only form of the proteinase detected in the lung during LPS-mediated acute lung injury (ALI) in mice (2). Collectively, these data suggest that membrane-bound MMP-8 and -9 are important bioactive forms of the proteinase *in vivo*. However, the mechanism by which MMP-8 and MMP-9 bind to PMN surfaces is not clear.

Human PMNs store preformed TIMP-1 protein within their cytoplasmic vesicles which are distinct from the specific and gelatinase granules in which proMMP-8 and proMMP-9 are stored, respectively (33). TIMP-1 that is freely released by degranulating PMNs (33) is thought to control the activity of MMPs released by activated PMNs. Herein, we tested the hypothesis that TIMP-1 is also expressed on the surface on PMNs after they degranulate and that membrane-bound TIMP-1 on PMNs regulates pericellular proteolysis. We now report a novel localization for TIMP-1 on the surface of activated human, non-human primate (NHP), and murine PMNs and neutrophil extracellular traps (NETs) released by activated cells. In addition, exposure of NHPs to CS for 4 weeks upregulates co-localized expression of TIMP-1 with MMP-8 and MMP-9 on the surface of peripheral blood PMNs. Surface-bound TIMP-1 on PMN promotes (rather than inhibits) pericellular proteolysis by serving as a receptor for active forms of MMP-8 and -9 on the surface of activated PMNs. Thus, surface-bound TIMP-1 may contribute to PMN-mediated tissue destruction that occurs in COPD, cystic fibrosis, and other diseases associated with neutrophilic inflammation.

MATERIALS AND METHODS

Materials:

Goat anti-rabbit $F(ab)_2$ conjugated to Alexa Fluor® 488, goat anti-rabbit $F(ab)_2$ conjugated to Alexa Fluor® 546, goat anti-mouse $F(ab)_2$ conjugated to Alexa Fluor® 488, and goat anti-mouse $F(ab)_2$ conjugated to Alexa Fluor® 546, dye quenched (DQ) FITC-conjugated gelatin, DQ-FITC conjugated type I collagen and SYTOX™ Blue Nucleic Acid Stain were obtained from Invitrogen Life Technologies (Carlsbad, CA). Purified murine Timp-1, murine Timp-2, murine Mmp-8, and murine Mmp-9 proteins were purchased from R & D Systems (Minneapolis, MN). Full length murine Mmp-8 (residues 21–465) and murine Mmp-9 (residues 20–730) proteins and mutant murine Mmp-8 (residues 21–276) and murine Mmp-9 (residues 20–519) proteins containing the catalytic domains and hinge regions but lacking the COOH-terminal hemopexin domains were obtained from Abnova (Taipei City, Taiwan). (7-Methoxycoumarin-4-yl)-Acetyl-Pro-Leu-Gly-Leu-(3-[2,4-dinitrophenyl]-L2,3-diaminopropionyl)-Ala-Arg-NH_2 (McaPLGLDpaAR) was purchased from CalBiochem Novabiochem Corp. (San Diego, CA). Murine hemopexin protein was purchased from Sino Biological (Wayne, PA).

Antibodies:

Polyclonal rabbit anti-human MMP-9 IgG (AB805), polyclonal rabbit anti-murine Mmp-9 IgG (AB19047), murine anti-human MMP-9 IgG (MAB13416), polyclonal rabbit anti-human MMP-8 IgG (AB8115), polyclonal rabbit anti-TIMP-1 IgG (AB800), and rabbit anti-

TIMP-2 IgG (AB771) were purchased from Millipore (Billerica, MA). Murine anti-TIMP-1 IgG was obtained from R & D Systems (Minneapolis, MN). Rabbit anti-murine Mmp-8 IgG and rabbit anti-murine Mmp-9 IgG were purchased from Abcam (Cambridge, MA)

Human studies:

All studies of human subjects were approved by the Partners Healthcare Institutional Review Board.

Animal studies:

All procedures performed on mice were approved by the Harvard Medical School Institutional Animal Care and Use Committee. All experiments conducted on non-human primates (NHPs) were approved by the LRRI Institutional Animal Care and Use Committee.

Human PMN isolation and activation:

PMNs were isolated from peripheral blood of healthy male and female human donors (34), and incubated for 30 min at 37°C in HBSS containing 10 mM HEPES (pH 7.4) with or without varying concentrations of phorbol myristate acetate (PMA), lipopolysaccharide (LPS), tumor necrosis factor-α (TNF-α), interleukin-8 (IL-8), IL-1β, IL-6, 1-O-hexadecyl-2-acetyl-sn-glycero-3-phosphorylcholine (platelet activating factor, PAF) and N-formyl-leucyl-methionyl-phenylalanine (fMLP), or cytochalasin B followed by fMLP. PMN were also primed for 15 min at 37°C with PAF and LPS, and then activated for 30 min with 10^{-7} M fMLP. To terminate the assays, PMN were fixed in PBS (pH 7.4) containing 3% paraformaldehyde and 0.5% glutaraldehyde (26) for 3 min at 4°C.

Murine PMN isolation and activation:

Timp-1$^{-/-}$ mice in a pure C57BL/6 background were obtained from Paul Soloway (Division of Nutritional Sciences; Cornell University; Ithaca, NY). *Mmp-8*$^{-/-}$ and *Mmp-9*$^{-/-}$ mice both in a pure C57BL/6 background were generated as described previously (25,26). *Mmp-8*$^{-/-}$ *x Mmp-9*$^{-/-}$ compound mutant mice were generated by crossing the single Mmp-deficient lines. The genotypes of the mice were confirmed using PCR-based genotyping protocols on DNA extracted from tail biopsies.

PMN were isolated from the bone marrow of male and female *Mmp-8*$^{-/-}$, *Mmp-9*$^{-/-}$, *Timp-1*$^{-/-}$, *Mmp-8*$^{-/-}$ *x Mmp-9*$^{-/-}$ compound mutant mice, or C57BL/6 wild type (WT) mice by positive selection for Ly6G using immunomagnetic beads (26). Murine PMN preparations were >85% pure, as assessed by differential counting of Wright stained cytocentrifuge preparations, and >99% viable as assessed by exclusion of trypan blue dye. Murine PMN were activated at 37°C for 15 min with PAF (10^{-6} M) followed by fMLP (10^{-6} M for 30 min); these concentrations of agonists are optimal for inducing cell surface expression of Mmp-8 and Mmp-9 on PMNs (25,26). PMN were fixed, washed, and immunostained for cell surface murine Mmp-8 or -9, as outlined below.

Immunostaining of human PMN for surface-bound pro and active forms of MMP-8 and -9 and TIMPs:

Human PMNs were immunostained for cell surface TIMP-1 or TIMP-2 (as a control) using polyclonal rabbit human anti-TIMP-1 IgG (AB800), rabbit anti-human TIMP-2 IgG (AB771), or non-immune rabbit IgG as a control (1 μg/10^6 cells) followed by goat anti-rabbit F(ab)$_2$ conjugated to Alexa Fluor 488®. To assess whether MMP-9 and TIMP-1 are co-localized on the surface of PMNs, human PMN were activated for 15 min with 10^{-8} M PAF followed by 10^{-8} M fMLP and then fixed. Cells were double immunostained with monoclonal murine anti-human MMP-9 IgG (MAB13416) or monoclonal murine anti-human MMP-8 IgG and goat anti-murine F(ab)$_2$ conjugated to Alexa 546 for MMP-9, and with rabbit polyclonal anti-human TIMP-1 IgG (AB800) and goat anti-rabbit F(ab)$_2$ conjugated to Alexa 488. The antibodies used to detect surface-bound MMPs recognize both the pro and active forms of MMP-8 or MMP-9. Cells were examined with a Leica TCSNT confocal laser scanning microscope (Leica Inc., Exton, PA) fitted with air-cooled argon and krypton lasers. Fluorescent confocal micrographs were recorded under fluorescent imaging by exposing cells to 568 nm light attenuated by an acusto tunable optical filter using a long-pass 590 nm filter to detect the Alexa 546-labeled MMP-9 and Alexa 488-labeled TIMP-1.

Steady state TIMP-1 mRNA levels in human PMNs stimulated with fMLP, IL-1β, or IL-6:

Human PMNs isolated from peripheral blood samples drawn from healthy donors were incubated with or without 10^{-7} M fMLP, 10^{-7} M IL-1β, or 10^{-7} M IL-6. Total RNA was isolated from the PMNs using a SurePrep TrueTotal RNA Purification Kit (Fisher Scientific, Fair Lawn, NJ), following the manufacturer's instructions, and 1 μg of RNA was reverse transcribed into cDNA using a High-Capacity cDNA Reverse Transcription Kit (Thermo Fisher Scientific, Carlsbad, CA). SYBR green-based real-time RT-PCR was used to measure *TIMP-1* steady state mRNA levels with primers from Invitrogen (Charlestown, MA), PPIA as the housekeeping gene, an AriaMx Real-time PCR machine (Agilent technologies, Santa Clara, CA), and the comparative threshold method (35,36).

Quantitation of Mmp-8 or Mmp-9 on the cell surface of murine PMN:

To quantify Mmp-9 immuno-reactivity on the surface of murine PMNs, PMNs were isolated from C57BL/6 WT and *Timp-1*$^{-/-}$ mice, and activated for 15 min with 10^{-6} M PAF and then for 30 min with 10^{-6} M fMLP. Cells were fixed (as described above), and immunostained for cell surface Mmp-8 and Mmp-9 using rabbit anti-murine Mmp-8 IgG and rabbit anti-murine rabbit anti-murine Mmp-9 IgG (AB19047) or non-immune rabbit IgG as a control (1 μg/10^6 cells) followed by goat anti-rabbit F(ab)$_2$ conjugated to Alexa Fluor 488. Cell surface immunofluorescence was quantified in arbitrary fluorescence units using incident light epifluorescence microscopy (Leica Inc., Exton, PA) and image analysis software (MetaMorph™ software, Universal Imaging Inc., West Chester, PA), and the data were corrected for non-specific staining, as described previously (26,37).

Competitive binding experiments:

To determine whether Mmp-8 and Mmp-9 share binding sites on PMNs, competitive binding experiments were conducted. PMNs were isolated from the bone marrow of *Mmp-8*$^{-/-}$ *x*

Mmp-9$^{-/-}$ mice, and resuspended in PBS at 2×10^8 cells/ml. Cells were incubated with 10^{-6} M PAF for 15 min and 10^{-6} M fMLP for 30 min to induce surface expression of Timp-1. Cells were then chilled to 4°C, and incubated with or without 50–400 nM exogenous murine proMmp-8 protein for 45 min at 4°C to permit binding of exogenous Mmp-8 to the cell surface. Exogenous murine proMmp-9 protein (100 nM) was then added and cells incubated for an additional 60 min at 4°C to permit binding of exogenous murine proMmp-9 protein to the PMN surface. PMNs were washed twice in PBS, and then fixed and immunostained with Alexa 488 for surface-bound Mmp-9 as described above. Other aliquots of the PAF- and fMLP-activated PMNs were chilled to 4°C, and then incubated with or without 50–400 nM exogenous murine proMmp-9 protein for 45 min at 4°C to permit binding of exogenous Mmp-9 to the cell surface. Exogenous Mmp-8 protein (100 nM) was then added, and cells incubated for an additional 60 min at 4°C to permit binding of exogenous Mmp-8 to the PMN surface. PMNs were washed twice in PBS, and then fixed and immunostained with Alexa 488 for surface-bound Mmp-8, as described above.

Measurement of Mmp-8 and Mmp-9 catalytic activity on the surface of murine PMNs:

WT, *Mmp-9*$^{-/-}$, and *Timp-1*$^{-/-}$ PMNs were isolated from the bone marrow of mice, and activated as described above. The cells were fixed, washed, resuspended in Tris buffered saline (TBS; 50 mM Tris containing 0.15 M NaCl and 0.02 M $CaCl_2$; pH 7.4), and incubated at 37°C for 30 min in triplicate (10^6 cells/assay) with 1 mM PMSF [to inhibit membrane-bound serine proteinases expressed by activated PMNs (37–39)], with or without 1 mM 1,10-phenanthroline [a synthetic inhibitor of MMPs which inhibits membrane-bound MMPs (25,26)], and then incubated for 3 h with 1.8 μM McaPLGLDpaAR (a synthetic quenched fluorogenic substrate for MMPs). Total cell surface-bound MMP activity was quantified as the 1,10 o-phenanthroline inhibitable, McaPLGLDpaAR-hydrolyzing activity in cell-free supernatant samples using fluorimetry (Hitachi F2500 fluorescence spectrophotometer, Hitachi Ltd., Tokyo, Japan; Ex λ 328nm, Em λ 393nm) as described previously (26).

To quantify cell surface gelatinase activity, fixed, activated PMNs from WT, *Mmp-8*$^{-/-}$, and *Mmp-9*$^{-/-}$ mice were incubated with 1 mM PMSF with or without 1 mM 1, 10-phenanthroline (as described above) and then incubated in triplicate (3×10^6 cells/assay) at 37°C for 6 h with 50 μg/ml dye quenched (DQ)-FITC-conjugated gelatin, and surface MMP-mediated gelatinase activity was quantified as the 1, 10-o-phenanthroline-inhibitable cleavage of FITC-conjugated gelatin in cell-free supernatant samples using fluorimetry (Ex λ 490nm and Em λ 520nm) as described previously (26).

To quantify cell surface type-I collagenase activity, equal numbers of fixed, activated PMN from the three genotypes (5×10^6 cells/assay) were incubated with 1 mM PMSF with or without 1mM 1, 10-phenanthroline (as described above) and then incubated in triplicate with 50 μg/ml DQ-FITC-conjugated type-I collagen for 18 h at 37°C. Surface MMP-mediated type-I collagenase activity was quantified as the 1, 10-o-phenanthroline-inhibitable cleavage of FITC-conjugated type-I collagen in cell-free supernatant samples using fluorimetry (Ex λ 490nm and Em λ 520nm) as described previously (25).

Quantitation of Mmp-8 and Mmp-9 stored in and released from unstimulated and activated WT vs. Timp-1$^{-/-}$ PMNs:

PMNs were isolated from the bone marrow of WT and *Timp-1*$^{-/-}$ mice, counted, and lyzed at 5×10^6 cells/ml in RIPA buffer containing 1 mM PMSF, 1 mM 1,10-o-phenanthroline, and mammalian protease inhibitor cocktail (Sigma-Aldrich) diluted 1:100 (to prevent proteolytic degradation of Mmps). Other aliquots of the cells were resuspended at 10^7 cells/ml in PBS and incubated at 37°C for 30 min with or without fMLP (10^{-6} M). Cell-free supernatants were harvested and 1 mM PMSF, 1 mM 1,10-o-phenanthroline, and mammalian protease inhibitor cocktail (Sigma-Aldrich) diluted 1:100 were added and samples were frozen to −80°C. Mmp-8 and Mmp-9 were quantified in cell extracts and cell-free supernatant samples using ELISAs. In addition, the forms of Mmps released by unstimulated and activated PMNs were assessed using western blotting. Briefly, samples were subjected to electrophoresis on 8% SDS-PAGE under reducing conditions, proteins transferred to PVDF membranes, and probed with polyclonal rabbit anti-murine Mmp-9 IgG (AB19047) or rabbit anti-murine Mmp-8 IgG (Ab19045), followed by goat anti-rabbit IgG conjugated to horse radish peroxidase (Biorad, Hercules, CA), and a chemiluminescence detection system following the manufacturer's instructions.

Binding of exogenous Mmp-9 and Mmp-8 to murine PMNs and Timp-1 reconstitution experiments:

PMNs isolated from the bone marrow of *Mmp-9*$^{-/-}$, *Mmp-8*$^{-/-}$, and *Timp-1*$^{-/-}$ mice were activated at 37°C for 15 min with 10^{-6} M PAF followed by 10^{-6} M fMLP for 30 min to induce PMN degranulation and the release of Timp-1 from *Mmp-9*$^{-/-}$ and *Mmp-8*$^{-/-}$ PMNs and the subsequent binding of Timp-1 to the surface of these PMNs. PMNs were then washed and resuspended in cold HBSS containing 10 mM HEPES (pH 7.4) or 50 mM Tris containing 0.15 M NaCl and 0.02 M $CaCl_2$; pH 7.4. The *Mmp-9*$^{-/-}$, *Mmp-8*$^{-/-}$, and *Timp-1*$^{-/-}$ PMNs were then incubated at 4°C with or without 50–400 nM purified murine proMmp-9 or proMmp-8 at 4°C for 90 min. In other experiments, *Timp-1*$^{-/-}$ PMNs were incubated at 4°C for 60 min with or without 200 nM Timp-1 protein (or 200 nM Timp-2 protein or 200 nM myeloperoxidase protein, as controls). Cells were washed twice, incubated at 4°C for 60 min with or without 200 nM proMmp-8 or 200 nM proMmp-9, and PMNs were then washed and fixed. Mmp-8 and Mmp-9 that bound to cells was detected by immunostaining the cells with Alexa-488 for Mmp-8 or Mmp-9, as described above. Mmp-8 and Mmp-9 that bound to cells was also quantified as the PMN surface-associated cleavage of susceptible substrates that were conjugated to quenched FITC (type I collagen for Mmp-8 or gelatin for Mmp-9) in the presence of amino-phenyl mercuric acetate (1 mM APMA; Sigma, St. Louis, MO) using TBS as the assay buffer and fluorimetry (Ex λ 490nm and Em λ 520nm) as described previously (26).

Binding of full length versus mutant proMmps lacking the COOH terminus hemopexin domains to PMNs from Mmp-8$^{-/-}$ x Mmp-9$^{-/-}$ compound mutant mice

Full length proMmp-9 (FL proMmp-9; residues 20–730) or 400 nM full length proMmp-8 (FL proMmp-8; residues 21–465), or 400 nM mutant proMmp-9 lacking only the COOH terminal hemopexin domain (MT Mmp-9; residues 20–519), or mutant proMmp-8 protein

lacking only the COOH terminal hemopexin domain (MT proMmp-8; residues 21–276) were obtained from Abnova (Teipei City, Tiawan). To confirm that these latent proMMPs have catalytic activity when activated, 50 nM FL proMmp-8, FL proMmp-9, MT proMmp-8, or MT proMmp-9 proteins in Tris assay buffer were activated by adding 1 mM pamino-phenyl mercuric acetate (APMA; Sigma, St. Louis, MO), and incubating the samples at 37°C for 8 h (for FL and MT proMmp-8) or 18 h (for FL and MT proMmp-9). The samples were then incubated at 37°C in duplicate for up to 18 h with 2 μM McaPLGLDpaAR, and cleavage of this substrate was quantified using fluorometry, as described above.

PMNs isolated from *Mmp-8*$^{-/-}$ *x Mmp-9*$^{-/-}$ mice were activated at 37°C for 15 min with PAF (10^{-6} M) and then for 30 min with fMLP (10^{-6} M) to induce Timp-1 surface expression. The PMNs were then incubated at 4°C for 2 h with or without 400 nM FL proMmp-9, 400 nM FL proMmp-8, 400 nM MT proMmp-9, or 400 nM MT Mmp-8. Bound Mmp-9 and Mmp-8 were detected by immunostaining cells with Alexa 488 using an antibody raised to the hinge region of Mmp-9 or Mmp-8 (which was present in both the MT and FL forms of Mmp-8 and Mmp-9), as described above.

Competition experiments with soluble hemopexin:

PMNs isolated from *Mmp-8*$^{-/-}$ *x Mmp-9*$^{-/-}$ mice were activated at 37°C for 15 min with PAF (10^{-6} M) and then for 30 min with fMLP (10^{-6} M) to induce Timp-1 surface expression. The PMNs were then incubated at 4°C for 60 min with or without 500 nM purified murine hemopexin protein (Sino Biological, Wayne, PA), and then incubated at 4°C for 60 min with or without 400 nM proMmp-8 (R&D Systems, Minneapolis, MN) or 400 nM proMmp-9 (R&D Systems, Minneapolis, MN). Cells were then washed, fixed, and Mmp-8 and Mmp-9 that bound to cells was quantified by immunostaining the cells with Alexa-488 for Mmp-8 or Mmp-9, as described above.

Isolation and staining of neutrophil extracellular traps (NETs) for TIMP-1, MMP-8, and MMP-9:

Human PMNs suspended in RPMI medium were dispensed into 8-well chamber slides and incubated with or without 1 μg/mL of LPS from *Escherichia coli* 0111:B4 for 4 h at 37°C to induce NET formation (40). PMN cell-free supernatant samples were removed, and PMNs and NETs attached to the chamber slide were fixed in PBS (pH 7.4) containing 3% paraformaldehyde and 0.5% glutaraldehyde. NETs in the supernatant samples were identified by staining for extracellular DNA using SYTOX™ Blue Nucleic Acid Stain (Invitrogen) following the manufacturer's instructions. PMN-associated NETs were immunostained with either rabbit polyclonal anti-human MMP-9 IgG (Abcam) and goat anti-rabbit $F(ab)_2$ conjugated to Alexa-546, or rabbit polyclonal anti-human MMP-8 IgG (Abcam) and goat anti-rabbit $F(ab)_2$ conjugated to Alexa-546. The preparations were then stained with murine monoclonal anti-human TIMP-1 IgG (Invitrogen Life Technologies, Carlsbad, CA) and goat anti-mouse $F(ab)_2$ conjugated to Alexa-488. PMN-associated NETs were examined and images of the cells acquired using a confocal laser scanning microscope, as described above.

NHP CS Exposures:

As described previously, the NHPs were socially housed (up to two animals per cage) in the Primate Facility at the Lovelace Respiratory Research Institute (Albuquerque, NM), in accordance with the Guide for Laboratory Animal Practice under the Association for the Assessment and Accreditation for Laboratory Animal Care International–approved animal environmental conditions (41). NHPs were exposed to 100% freshly filtered air with 10 to 15 air changes per hour in the control and cigarette smoke (CS) exposure group before initiating the exposures (41). NHPs were exposed to CS [250 mg/m^3 total suspended particulate matter (TPM)] in H2000 whole body exposure chambers for 6 h-per-day, 5 days-per-week for 4 weeks, as described previously (41), to simulate a heavy human smoking pattern. For a 3 Kg NHP inhaling an average volume of 800 ml/minute, a pulmonary TPM deposition of 20%, the weekly deposition of smoke particles would be ~ 2.9 or 7.2 TPM deposited per gram of lung per week, as calculated previously (41). Assuming that a human smoker smoking an average of 20 cigarettes per day for 1 week will have 1.8 mg TPM deposited per gram of lung per week, the 100 and 250 mg/m^3 TPM CS dose for NHPs is similar to that of humans smoking approximately 1.8 or 4 packs per day, respectively (41). Control NHPs were exposed to air for 4 weeks.

PMN isolation from NHPs and immunostaining for surface-bound MMP-8, MMp-9 and TIMP-1:

Arterial blood samples were collected (10 ml/time point) using a heparinized needle and syringe. PMNs were separated from the mononuclear cell (MNC) fraction by density gradient centrifugation using Lymphoprep (STEMCELL Technologies, Cambridge, MA). Red blood cells were removed from the granulocyte fraction by dextran sedimentation followed by hypotonic lysis. The PMNs were immediately fixed in PBS containing 3% paraformaldehyde and 0.25% glutaraldehyde for 5 min on ice and then washed, and resuspended in cold PBS containing 1% albumin and 50 μg/ml goat IgG to block non-specific binding of antibodies to Fc receptors. The PMNs were then immunostained with either rabbit polyclonal anti-human MMP-9 IgG (Abcam) and goat anti-rabbit $F(ab)_2$ conjugated to Alexa-546, or rabbit polyclonal anti-human MMP-8 IgG (Abcam) and goat anti-rabbit $F(ab)_2$ conjugated to Alexa-546. The cells were then double immunostained with murine monoclonal anti-human TIMP-1 IgG (Invitrogen Life Technologies, Carlsbad, CA) and goat anti-mouse $F(ab)_2$ conjugated to Alexa-488. PMNs were examined with a confocal laser scanning microscope and images of the cells were acquired as described above. Cell surface immunofluorescence was quantified using image analysis software (MetaMorph™ software, Universal Imaging Inc., West Chester, PA), and the data were corrected for non-specific staining, as described previously (26,37).

Statistics:

The results for paired and unpaired data were compared using the Student’s t-test for parametric data and the Mann-Whitney rank sum U test for non-parametric data; $P < 0.05$ was considered significant.

RESULTS

TIMP-1 is expressed in an inducible manner on the surface of human PMNs:

TIMP-1 is stored in PMN cytoplasmic vesicles which translocate to the PMN plasma membrane when PMNs are incubated with phorbol ester to induce PMN degranulation (33). To test the hypothesis that TIMP-1 is expressed on the surface of PMNs when they degranulate, non-permeabilized human PMNs that had been activated with a degranulating agonist (fMLP) for 30 min were immunostained for surface-bound TIMP-1 and examined using confocal microscopy. There was intense staining for TIMP-1 on the surface of fMLP-activated PMNs which was frequently localized to the leading edge of the cells (Fig. 1A). However, there was minimal surface fluorescence associated with cells incubated with an isotype-matched control primary antibody, as expected (Fig. 1A). Quantitative analysis of unstimulated vs. activated PMNs demonstrated minimal staining for TIMP-1 on the surface of unstimulated PMN, but robust staining for TIMP-1 on the surface of fMLP-activated PMNs (Fig. 1B). As a control, fMLP-activated PMNs were immunostained with an antibody to TIMP-2 [as TIMP-2 is not expressed by PMNs (13,42)]. As expected, surface staining for TIMP-2 was not detected on fMLP-activated PMNs (Fig. 1B). FMLP also increased surface Timp-1 expression on PMNs isolated from wild type (WT) mice (Fig. 1C). To confirm the specificity of the anti-Timp-1 antibody, unstimulated and fMLP-activated PMNs from *Timp-1*$^{-/-}$ mice were immunostained for surface Timp-1 using this antibody. No staining was detected, as expected (Fig. 1C). Thus, activation of human and murine PMNs with the degranulating agonist, fMLP, induces rapid translocation of TIMP-1 to the cell surface.

Degranulating agonists potently and rapidly up-regulate surface TIMP-1 levels on PMN:

We assessed whether other degranulating agonists that vary in the potency with which they induce PMN degranulation vary correspondingly in the potency with which they induce surface expression on TIMP-1 on PMNs. Pharmacologic agonists that potently induce PMN degranulation including phorbol ester and a calcium ionophore (A23187) induced substantially greater increases in surface TIMP-1 levels on PMNs than biologic mediators (fMLP and TNF-α) that have more modest potency in inducing PMN degranulation (Fig. 2A). The effects of fMLP on PMN surface TIMP-1 levels were concentration-dependent, and the optimal fMLP concentration (10^{-7} M) induced ~20-fold increases in surface TIMP-1 staining versus that detected on the surface of unstimulated PMNs (Fig. 2B). The effects of fMLP were also very rapid. Significant increases in surface-bound TIMP-1 were detected within 5 min of adding fMLP to the cells, and optimal increases occurred after 30 min (Fig. 2C). Significant increases in surface TIMP-1 persisted for at least 90 min after adding fMLP (Fig. 2C) and returned to baseline 2 h after adding fMLP to the cells (not shown). Other pro-inflammatory mediators (LPS, PAF, TNF-α, IL-8, IL-1β, and IL-6) also rapidly increased surface-bound TIMP-1 levels on PMN, but less potently than fMLP (Fig. 2D–2E). The effects of IL-8 on PMN surface TIMP-1 levels were also concentration-dependent, and 10^{-8} to 10^{-6} M IL-8 induced maximal ~8-fold increases in surface TIMP-1 staining (Fig. 2F). However, agonists (fMLP, IL-1β and IL-6) did not increase surface TIMP-1 levels by *TIMP-1* gene expression in PMNs as unstimulated and PMNs activated with these agonists had similar *TIMP-1* steady state mRNA levels as assessed by qRT-PCR (Supplemental Fig. 1). Priming PMNs with LPS, TNF-α, or PAF, and then activating them fMLP induced

additive effects on cell surface expression of serine proteinases and MMPs on PMNs (25,26,37–39). Thus, the effects of priming PMNs with cytokines and bacterial products and then activating them with fMLP on surface TIMP-1 levels were studied. Priming PMNs with LPS, PAF, or TNF-α and then activating them with the optimal concentration of fMLP did not further increase surface TIMP-1 levels on PMN when compared with the effects of fMLP alone (Fig. 2D).

Co-localization of TIMP-1 and MMPs on PMN surfaces:

Soluble TIMP-1 binds to and inhibits soluble forms of MMP-8 and MMP-9. Thus, we tested the hypothesis that surface-bound TIMP-1 expressed on activated PMNs anchors active MMPs to the PMN surface. First, we assessed whether MMPs and TIMP-1 are co-localized on the surface of activated PMNs by double immunostaining fMLP-activated human PMNs with a red fluorophore for surface MMP-8 or -9 and a green fluorophore for surface TIMP-1. Analysis of the double immunostained cells using confocal microscopy confirmed that MMP-9 and TIMP-1 (Fig. 3A) and MMP-8 and TIMP-1 (Fig. 3B) were strikingly co-localized on the surface of activated PMNs (especially at the leading edges of the cells). Minimal staining was detected on the surface of unstimulated PMNs (Supplemental Fig. 2) or cells stained with non-immune isotype matched control primary antibodies (Fig. 3C).

ProMmp-8 and Mmp-9 share binding sites on the surface of PMNs:

We tested the hypothesis that proMmp-8 and -9 bind to the same binding sites on the PMN surface. First, we performed competition experiments in which we tested whether pre-incubating activated murine PMNs with purified exogenous proMmp-8 protein blocks the subsequent binding of exogenous proMmp-9 to the cells (and vice versa). PMNs isolated from *Mmp-8*$^{-/-}$ *x Mmp-9*$^{-/-}$ mice were used in these experiments as these cells lack endogenous proMmp-8 and proMmp-9 which would compete with exogenous proMmps for binding sites on PMNs. Preliminary experiments confirmed that Timp-1 (our putative binding site for Mmps on PMNs) is expressed on the surface of PMNs from *Mmp-8*$^{-/-}$ *x Mmp-9*$^{-/-}$ mice. Significantly greater amounts of Timp-1 were detected on the surface of *Mmp-8*$^{-/-}$ *x Mmp-9*$^{-/-}$ PMNs than PMNs from WT mice (Supplemental Fig. 3). This is likely due to the lack of binding of endogenous proMmps to surface-bound Timp-1 thereby increasing the access (and binding) of anti-Timp-1 IgG to surface-bound Timp-1 on PMNs. Pre-incubating activated *Mmp-8*$^{-/-}$ *x Mmp-9*$^{-/-}$ PMNs with exogenous proMmp-8 (Fig. 4A) or exogenous proMmp-9 (Fig. 4B) inhibited the subsequent binding of exogenous proMmp-9 (Fig. 4A) or proMmp-8 (Fig. 4B), respectively, to the PMN surface in a concentration-dependent manner. These results support the hypothesis that proMmp-8 and -9 share binding sites on the surface of activated PMNs.

Timp-1 is required for the binding of active Mmp-8 and Mmp-9 to PMNs:

To investigate whether membrane-bound Timp-1 on activated PMNs binds Mmp-8 and Mmp-9 to PMNs, we immunostained activated PMNs from WT or *Timp-1*$^{-/-}$ mice (or *Mmp-8*$^{-/-}$ or *Mmp-9*$^{-/-}$ mice as negative controls) for surface-bound pro and active forms of Mmp-8 or Mmp-9 using antibodies that bind to the hinge regions of the Mmps (which are present in both pro and active forms of the Mmps). In contrast to activated WT PMNs, activated *Timp-1*$^{-/-}$ PMNs lacked immuno-reactive pro and active Mmp-8 (Fig. 5A) and

Mmp-9 (Fig. 5B) on their cell surface as did activated PMNs from *Mmp-8*$^{-/-}$ and *Mmp-9*$^{-/-}$ mice (as expected).

To assess whether *Timp-1*$^{-/-}$ PMNs also lack active forms of Mmp-8 on their surface, we performed loss-of-function studies in which we compared PMN cell surface MMP activity associated with equal numbers of WT vs. *Timp-1*$^{-/-}$ fixed, activated PMNs against substrates that are highly susceptible to cleavage by active Mmp-8 (type-I collagen) or active Mmp-9 (gelatin). Our prior studies (25,26) confirmed that: 1) fixing PMNs prevents free release of Mmps from the cells thereby eliminating the contributions of Mmps released by the cells to substrate cleavage; 2) the fixation process used has a minimal effect on the catalytic activity of surface-bound Mmps; 3) surface-bound Mmp-8 on activated WT murine PMNs accounts for the majority (~90%) of Mmp-mediated cell surface collagenase activity expressed by activated WT PMNs (25); and 4) surface-bound Mmp-9 on PMNs accounts for the majority (~70%) of the Mmp-mediated cell surface gelatinase activity on activated WT PMNs (26). *Timp-1*$^{-/-}$ *and Mmp-8*$^{-/-}$ PMNs had similar (~75%) reductions in surface type-I collagenase activity (indicative of loss of surface Mmp-8 activity) when compared with that associated with activated WT murine PMNs (Fig. 5C). Also, *Timp-1*$^{-/-}$ PMNs and *Mmp-9*$^{-/-}$ PMNs had similar (~70–80%) reductions in surface gelatinase activity (indicative of loss of surface Mmp-9 activity) when compared with activated WT PMNs (Fig. 5D). As a negative control, we also studied gelatinase activity associated with *Mmp-8*$^{-/-}$ PMN as our previous studies showed that surface Mmp-8 present on activated PMNs has no significant gelatin-degrading activity (25). There was no significant reduction in surface Mmp-mediated gelatinase activity associated with *Mmp-8*$^{-/-}$ PMNs as expected (Fig. 5D).

We also compared the surface-bound Mmp activities of equal numbers of fixed activated WT and *Timp-1*$^{-/-}$ PMNs against a quenched fluorogenic substrate which is susceptible to cleavage by both Mmp-8 and Mmp-9 (McaPLGLDpaAR). *Timp-1*$^{-/-}$ PMNs had significantly less McaPLGLDpaAR-cleaving activity than either *Mmp-8*$^{-/-}$ or *Mmp-9*$^{-/-}$ PMNs consistent with the notion that Timp-1 serves as the receptor for both Mmp-8 and Mmp-9 on PMN surfaces (Fig. 5E). Thus, *Timp-1*$^{-/-}$ PMN have substantial reductions in both immunoreactive and active forms of Mmp-8 and Mmp-9 on their surface.

Timp-1$^{-/-}$ PMNs contain and release similar quantities of Mmp-8 and Mmp-9 as WT PMNs:

We considered the possibility that the lack of Mmp-8 and Mmp-9 on the surface of activated *Timp-1*$^{-/-}$ PMNs was due to the impaired production, release, or stability of Mmp-8 and Mmp-9 that are expressed by PMNs that are deficient in Timp-1. Thus, the quantities of proMmp-8 and proMmp-9 contained within equal numbers of unstimulated WT and *Timp-1*$^{-/-}$ PMNs and the quantities of Mmp-8 and Mmp-9 released by equal numbers of activated WT and *Timp-1*$^{-/-}$ PMNs were measured using ELISAs. Extracts of unstimulated *Timp-1*$^{-/-}$ PMNs contained similar amounts of Mmp-9 and Mmp-8 as WT PMNs (Tables 1 and 2 and Fig. 6). FMLP-activated *Timp-1*$^{-/-}$ PMNs also freely released similar quantities of Mmp-9 and Mmp-8 (Tables 1 and 2 and Fig. 6) as WT PMNs. Both Mmps were released from WT and *Timp-1*$^{-/-}$ PMNs exclusively as proMmps as assessed by western blotting, as expected (Fig. 6). These results indicate that the lack of Mmp-8 and Mmp-9 on the surface

of activated *Timp-1*$^{-/-}$ PMNs is not due to impaired production, release, or stability of these Mmps when PMNs lack Timp-1.

Exogenous Timp-1 reconstitutes the binding of exogenous Mmp-8 and -9 to Timp-1$^{-/-}$ PMNs:

Next, we assessed whether the binding of proMmp-8 or proMmp-9 to PAF- and fMLP-activated *Timp-1*$^{-/-}$ PMNs can be reconstituted by incubating these cells with exogenous murine proMmp-8 or proMmp-9, respectively. PMN incubations were conducted at 4°C to minimize internalization of bound proteinases. The binding of exogenous proMmp-8 or proMmp-9 proteins to PAF- and fMLP-activated *Mmp-8*$^{-/-}$ or *Mmp-9*$^{-/-}$ PMNs at 4°C was also measured as a positive control as *Mmp-8*$^{-/-}$ and *Mmp-9*$^{-/-}$ PMNs express Timp-1 on their surface in an inducible manner (data not shown) but lack endogenous Mmp-8 and Mmp-9, respectively. Exogenous proMmp-8 and proMmp-9 proteins bound to the surface of activated *Mmp-8*$^{-/-}$ or *Mmp-9*$^{-/-}$ PMNs, respectively, in a concentration-dependent manner but did not bind to the surface of activated *Timp-1*$^{-/-}$ PMNs even when high (400 nM) concentrations of exogenous proMmps were tested (Figs. 7A and 7B).

Next, reconstitution experiments were performed in which *Timp-1*$^{-/-}$ PMNs were incubated with or without exogenous Timp-1 protein or control proteins including: 1) exogenous Timp-2 which is not a PMN product (13); or 2) myeloperoxidase (MPO) which is a PMN product that binds to PMN surfaces following PMN degranulation (43). These assays were performed at 4°C to permit binding of these proteins to the surface of PMN while minimizing their internalization. Unbound exogenous proteins were removed by washing the cells, and the PMNs were then incubated with exogenous proMmp-8 or proMmp-9. ProMmps that bound to the cells were quantified either by immunostaining the cells for Mmp-8 or Mmp-9, or by measuring surface levels of active Mmp-8 or Mmp-9 by quantifying PMN surface-associated cleavage of susceptible substrates (quenched FITC-conjugated type I collagen for Mmp-8 or quenched FITC-conjugated gelatin for Mmp-9). Only *Timp-1*$^{-/-}$ PMNs that had first been incubated with exogenous Timp-1 protein were then able to bind exogenous proMmp-8 or proMmp-9 to their surface as assessed by immunostaining experiments (Figs. 7C and 7D). PMN surface-associated type-I collagenase and gelatinase assays confirmed that the binding of exogenous Timp-1 protein to the surface of *Timp-1*$^{-/-}$ PMNs reconstituted the binding of exogenous Mmp-8 and Mmp-9 proteins to these cells (Fig. 7E–7F). These data support the notion that membrane-bound Timp-1 anchors Mmp-8 and Mmp-9 to the surface of PMNs and thereby may contribute to pericellular collagenase and gelatinase activity.

Binding of full length (FL) versus mutant (MT) forms of proMmp-8 and proMmp-9 lacking the COOH hemopexin domains to surface-bound Timp-1 on PMNs:

Next, we tested the hypothesis that the COOH terminal hemopexin domains of proMmp-8 and proMmp-9 mediate the binding of these proMmps to surface-bound Timp-1 that is expressed on activated PMNs. The rationale for this hypothesis is that the binding of the proMmps *via* their COOH terminal domains to surface-bound Timp-1 would leave the NH_2-terminal pro-domains free to be activated in the extracellular space and also permit the catalytic domain adjacent to the pro-domain to cleave extracellular substrates [such as type I

collagen and gelatin (see Figs 5C and 5D)]. To test this hypothesis, we compared the binding of recombinant FL proMmp-8 and proMmp-9 vs. MT forms of these proMmps (that lack only the COOH-terminal hemopexin domains of the Mmps) to activated *Mmp-8*$^{-/-}$ *x Mmp-9*$^{-/-}$ PMNs. PMNs from *Mmp-8*$^{-/-}$ *X Mmp-9*$^{-/-}$ mice were studied as these cells express Timp-1 on their surface in an inducible fashion but lack endogenous Mmp-8 and Mmp-9 which would compete with exogenous proMmps for binding to surface-bound Timp-1. Initial experiments confirmed that the recombinant FL and MT proMmp-8 and pro-Mmp-9 proteins retained their capacity not only to be activated with APMA, but also to degrade a sensitive peptide substrate for Mmps (McaPLGLDpaAR; Supplemental Fig. 4). Degradation of this substrate by the MT forms of both APMA-activated Mmp-8 and Mmp-9 was less efficient when compared with that mediated by the activated FL forms, which is consistent with prior studies showing that the COOH terminal domains are crucial for efficient substrate cleavage by binding Mmps to their susceptible substrates (44). FL proMmp-8 and proMmp-9 bound avidly to *Mmp-8*$^{-/-}$ *x Mmp-9*$^{-/-}$ PMNs. However, COOH-truncated MT forms of both proMmp-8 and proMmp-9 lacking the hemopexin domains failed to bind to *Mmp-8*$^{-/-}$ *x Mmp-9*$^{-/-}$ PMNs (Figs. 8A and 8B). Pre-incubating activated *Mmp-8*$^{-/-}$ *x Mmp-9*$^{-/-}$ PMNs with soluble exogenous hemopexin also efficiently inhibited the binding of exogenous proMmp-8 and proMmp-9 proteins to these cells (Figs. 8C and 8D). Thus, the COOH-terminal hemopexin domains are required for proMmp-8 and proMmp-9 to bind to membrane-bound Timp-1 expressed on activated PMNs.

Co-localization of TIMP-1 and MMPs in PMN extracellular traps (NETs):

NETs are a meshwork of chromatin fibers that contain PMN granule-derived peptides and proteinases and are extruded by PMNs activated with LPS and other agonists (45). NETs trap and promote killing of pathogens, but can contribute to tissue injury in various organs (45). NETs contain MMP-8, MMP-9, and MMP-25 following their released from PMN granules and vesicles (40,46), but it is not known whether NETs contain TIMP-1 or whether MMP-8 and MMP-9 form complexes with TIMP-1 in NETs. NET release was induced by incubating human PMNs with LPS for 4 h (Figs. 9A and 9B), and cell-associated NETs were double-immunostained for TIMP-1 and either MMP-8 or MMP-9. TIMP-1 was present in NETs that were released by activated PMNs, and TIMP-1 co-localized with both MMP-8 and MMP-9 that were present in NETs (Fig. 9A).

Exposing NHPs to cigarette smoke (CS) increases surface TIMP-1, MMP-8, and MMP-9 staining on peripheral blood PMNs and induces co-localization of TIMP-1 with MMP-8 and MMP-9 on PMN surfaces:

MMP-8 and MMP-9 are elevated in blood and/or lung samples from smokers and patients with COPD (47,48), and these MMPs have been strongly implicated in emphysema development occurring in COPD (49). We recently described a novel NHP model of CS-induced acute lung pathologies in which CS exposures are similar to those experienced by human heavy cigarette smokers [2–4 packs per day (41)]. Also, lung levels of MMPs were increased in CS-exposed NHPs (41). Thus, we evaluated whether exposing NHPs to CS leads to: 1) increased expression of TIMP-1, MMP-8, and MMP-9 on the surface of peripheral blood PMNs; and 2) co-localization of TIMP-1 with MMP-8 and MMP-9 on PMN surfaces. NHPs were exposed to air or CS for 4 weeks, PMNs were isolated from

blood samples drawn from each NHP at baseline and immediately after the last air or CS exposure, and PMNs were double immunostained for surface-bound TIMP-1 and either MMP-8 or MMP-9.

There was minimal staining for TIMP-1, MMP-8, or MMP-9 on the surface of peripheral blood PMNs isolated from NHPs either at baseline or after 4 weeks of air exposure (Fig. 10A, 10C, 10D, and 10E). Exposure of NHPs to CS for 4 weeks upregulated surface TIMP-1, MMP-8, and MMP-9 protein levels on peripheral blood PMNs (Fig. 10B, 10C, 10D, and 10E). In addition, surface TIMP-1 was co-localized with surface MMP-8 and MMP-9 staining on PMNs from CS-exposed NHPs (Fig. 4B).

DISCUSSION

Herein, we report a novel localization for TIMP-1 on the surface of activated human and murine PMNs. In contrast to soluble TIMP-1 (which is an important inhibitor of soluble forms of active MMP-8 and -9), membrane-bound TIMP-1 on PMNs plays a counterintuitive role in promoting (rather than inhibiting) MMP-8 and MMP-9-mediated proteolysis in the pericellular environment of activated PMN by anchoring MMP-8 and MMP-9 to the PMN surface *via* their COOH-terminal hemopexin domains. PMNs release NETs when activated, and TIMP-1 co-localized with both MMPs that were present in NETs indicating that TIMP-1 may also anchor MMP-8 and MMP-9 to NETs to promote MMP-mediated tissue injury. In addition, exposure of NHPs to CS upregulated co-localized expression of TIMP-1 with MMP-8 and MMP-9 on peripheral blood PMNs. Thus, membrane-bound TIMP-1 may contribute to PMN MMP-mediated extracellular matrix degradation and tissue destruction that occurs in COPD, cystic fibrosis and other diseases characterized by neutrophilic inflammation (49–51).

Multiple lines of evidence support the notion that surface-bound TIMP-1 serves as a common receptor for pro and active forms of MMP-8 and MMP-9 on PMNs including: 1) the strong colocalization of TIMP-1 with MMP-8 and MMP-9 often on the leading edge of polarized human PMNs; 2) the substantial reductions in immunoreactive pro and active Mmp-8 and Mmp-9 on the surface of activated *Timp-1*$^{-/-}$ murine PMNs; 3) the substantial reductions in PMN surface Mmp-8 activity (type-1 collagenase activity) and PMN surface Mmp-9 activity (gelatinase activity) that was associated with activated *Timp-1*$^{-/-}$ PMNs; 4) exogenous Timp-1 (but not Timp-2) protein reconstitutes the binding of exogenous immunoreactive and active Mmp-8 and -9 to activated *Timp-1*$^{-/-}$ PMNs; and 4) competition binding experiments using exogenous proMmp-8 and proMmp-9 protein confirming that these Mmps share binding sites on PMNs.

Price *et al.* first demonstrated that human PMNs store preformed TIMP-1 protein within cytoplasmic vesicles from where it is freely released when PMNs are activated with the pharmacologic agonist, phorbol ester (33). In the current study, we build on this literature by showing that biologically-relevant mediators that PMNs encounter at sites of inflammation induce robust increases in surface-bound TIMP-1. Price *et al.* did not investigate the function of TIMP-1 that is freely released by PMNs. Our study is the first to report that: 1) TIMP-1 is expressed on the surface of a leukocyte; and 2) TIMP-1 regulates the function of a leukocyte

(pericellular proteolysis). We have shown that TIMP-1 is expressed on the surface of activated human monocytes and murine macrophages (unpublished data, not shown) suggesting that surface-bound TIMP-1 may regulate the function of leukocytes other than PMNs. Soluble TIMP-1 binds to the surface of breast cancer cell lines and hematopoietic stems cells *in vitro* (52,53). TIMP-1 that binds to the surface of hematopoietic stem cells activates β1 integrins to increase cellular adhesion and migration (52). Exogenous TIMP-1 that binds to the surface breast cancer cell lines inhibits apoptosis of these cells *in vitro* (53). Whether surface-bound TIMP-1 regulates PMNs functions other than pericellular proteolysis will be the focus of our futures studies. Our time course experiments indicate that TIMP-1 translocates to the surface very rapidly (within 5 min of adding fMLP to PMNs). This time course is more rapid than that (15 min) reported for MMP-8 and MMP-9 binding to PMN surfaces (25,26), and is entirely consistent with the known faster mobilization of the lighter cytoplasmic vesicles (in which TIMP-1 is stored) than the more dense (and thus slower to mobilize) specific and gelatinase granules in which MMP-8 and MMP-9 are stored (13,42). This sequence of degranulation events will permit TIMP-1 to bind to the PMN surface before the release of MMPs has occurred, and will facilitate efficient surface anchoring of proMMP-8 and proMMP-9 subsequently released from the specific and gelatinase granules of PMNs.

PMNs produce NETs within minutes after activation (45). NETs are a meshwork of chromatin fibers that bind granule-derived antimicrobial peptides and proteinases that are extruded when PMNs are activated (45). NETs trap and promote the killing of pathogens by concentrating PMN-released antimicrobial proteins in the extracellular space. However, NETs can also promote PMN cell death and tissue injury in various diseases characterized by neutrophilic tissue inflammation (45). To our knowledge, this is the first report that NETs contain TIMP-1, and that TIMP-1 co-localizes with both MMP-8 and MMP-9 present in NETs. Thus, TIMP-1 may anchor pro and active forms of MMP-8 and MMP-9 to NETs as well as PMN surfaces to promote tissue injury.

Herein, we investigated whether translocation of TIMP-1, MMP-8, and/or MMP-9 to the PMN surface occurs during an inflammatory disease. We studied a large animal model of early COPD as increased MMP levels have been detected in lung samples from smokers and patients with subclinical emphysema (48,54), and MMPs have been strongly implicated in the pathogenesis of COPD (49). Furthermore, the NHP model uses smoke exposures that are similar to those experienced by heavy human cigarette smokers (41). The results showed that TIMP-1, MMP-8, and MMP-9 are upregulated on the surface of peripheral blood PMNs from NHPs exposed to CS for 4 weeks, and that these molecules are co-localized on PMN surfaces. These data are consistent with those in our *in vitro* studies, and support the notion that surface-bound TIMP-1 may contribute to the pathogenesis of diseases characterized by neutrophilic tissue injury such as COPD, cystic fibrosis, and rheumatoid arthritis (49,50). In addition, surface-bound TIMP-1, MMP-8, and MMP-9 may have utility as new biomarkers of CS-induced lung injury.

Other surface receptors for MMPs on cell surfaces:

Stefanidakis *et al.* reported that proMMP-8 and proMMP-9 bind to β2 integrins on human PMN surfaces, but they found no role for β2 integrins in binding active forms of these MMPs (30). The latter study reported that proMMP-9 binds to the principal ligand binding site (the I-domain) of the CD11b chains of CD11b/CD18 integrins on PMNs (30,31). However, active MMP-9 present on the surface of activated PMN was shown not to not bind to this integrin, and PMN from patients with leukocyte adhesion deficiency (which lack β2 integrins) express normal amounts of active MMP-9 bound to their surface. These results indicate that other receptors are involved in anchoring active MMP-9 to the PMN surface. One possible unifying hypothesis for the findings of Stefanidakis *et al.* and those in the current study is that some of the proMMP-8 and proMMP-9 that are released by degranulating PMNs initially bind with relatively low affinity to β2 integrins, and this interaction followed rapidly by binding of the pro-MMPs to surface-bound TIMP-1 on PMNs (with subsequent activation of the surface-bound pro-MMPs).

Other MMPs lacking transmembrane domains bind to the surface of tumor cells *in vitro*. MMP-7 and MMP-12 (which are not produced by PMNs) bind to the lipid bilayers of bicelles, colon cancer cells, cell lines *in vitro* (55,56). However, whether these MMPs bind to phospholipids in plasma membranes of leukocytes which express these MMPs (such as macrophages) is not clear.

Prior studies have shown that MMP-2 (gelatinase A) is expressed on the surface of tumor cells and fibroblasts, and surface-bound MMP-2 contributes to tumor cell invasiveness and metastasis (57,58). ProMMP-2 binds to these cells by forming a ternary complex with TIMP-2 and MT1-MMP. Specifically, the COOH-terminal hemopexin domain of pro-MMP-2 binds to the COOH-terminal domain of TIMP-2 and the NH_2-terminal inhibitory domain of TIMP-2 binds to the active site of a transmembrane proteinase (MT1-MMP) (5,57,58). An adjacent TIMP-free MT-MMP molecule dimerizes with the MT1-MMP in the complex, and activates proMMP2 by cleaving its pro-domain (5,57,58). Subsequent studies showed that all other 5 members of the MT-MMP subfamily can bind TIMP-2 within this ternary complex and subsequently participate in the activation of proMMP-2. Until the current study, this was the only known example of a TIMP family member functioning as a receptor for an MMP on a cell surface. TIMP-2 does not anchor MMP-8 or MMP-9 to PMNs as TIMP-2 is not a PMN product (13,42) and we detected no TIMP-2 on PMN cell surfaces by immunostaining. Also, the binding of exogenous Timp-2 to *Timp-1*$^{-/-}$ PMNs did not reconstitute the binding of Mmp-8 or Mmp-9 to PMNs. Thus, we have identified a novel mechanism for the binding of MMP-8 and MMP-9 to PMNs.

Consistent with the proMMP-2-TIMP-2 binding paradigm on tumor cells and fibroblasts, the hemopexin domains of proMMP-8 and proMMP-9 are required for these MMPs to bind to TIMP-1 on PMN surfaces. This notion is supported by our findings that: 1) mutant forms of proMmp-8 and proMmp-9 lacking only the COOH-terminal hemopexin domain failed to bind to the surface of activated PMNs (unlike the full length forms of the proMMPs); and 2) incubating activated *Mmp-8*$^{-/-}$ and *Mmp9*$^{-/-}$ PMNs with exogenous soluble hemopexin blocked the binding of exogenous proMmp-8 and proMmp-9 to these PMNs. The binding of the COOH-terminal hemopexin domains of proMmp-8 and proMmp-9 to surface-bound

Timp-1 on activated PMNs would leave the NH_2-terminal pro domains of the proMmps free to be activated in the extracellular space, and also their catalytic domains free to bind and cleave susceptible extracellular substrates such as extracellular matrix proteins. Consistent with this binding paradigm, it is also noteworthy that: 1) activated PMNs from WT mice are associated with robust Mmp-mediated type-I collagenase whereas activated *Timp-1*$^{-/-}$ and *Mmp-8*$^{-/-}$ PMNs are not; and 2) activated WT murine PMNs are associated with robust Mmp-mediated gelatin-degrading activity whereas activated *Timp-1*$^{-/-}$ and *Mmp-9*$^{-/-}$ PMNs are not. Thus, proMmp-8 and proMmp-9 are activated and retain catalytic activity following their binding to surface-bound Timp-1 on PMNs.

The mechanism by which TIMP-1 binds to PMNs and the domains of TIMP-1 involved in this process are not clear. CD63 (a tetraspanin) expressed by tumor cell lines and hematopoietic stems cells binds TIMP-1 to the surface of these cells (52,59). Although PMNs express CD63 (60), this protein is contained in PMN azurophil granules and translocates from these granules to the cell surface when PMNs are activated (13,42). However, as azurophil granules translocate to the PMN surface even more slowly than the secondary and tertiary granules which, in turn, translocate to the cell surface more slowly than the cytoplasmic vesicles in which TIMP-1 is stored, it is unlikely that CD63 anchors the TIMP-1 that appears on the PMN surface as early as 5 minutes after adding a degranulating agonist. It is noteworthy that TIMP-1 binds to and inhibits the catalytic activity of MT6-MMP (MMP-25), which is the only MT-MMP family member that is expressed by PMNs (61). Our preliminary experiments show that MT6-MMP is co-localized with TIMP-1 on fMLP-activated PMNs (unpublished results, not shown). A prior study reported that MMP-25 is present in NETs (40), raising the possibility that TIMP-1 anchors MMPs to PMN surfaces and NETs by binding to MMP-25 which will be investigated in our future studies. Whether the hemopexin domains of proMmp-8 and proMmp-9 bind to the COOH-terminal domain of TIMP-1 and the NH_2 terminal inhibitory domain of TIMP-1 binds to MT6-MMP on PMNs (similar to the MMP-2-TIMP-1-MT-MMP binding paradigm on tumor cells and fibroblasts) will be the focus of our future studies.

There is indirect evidence that Timp-1 anchors the active forms of Mmp-8 and Mmp-9 *in vivo* as *Timp-1*$^{-/-}$ mice phenocopy *Mmp-8*$^{-/-}$ and *Mmp9*$^{-/-}$ mice in several models of tissue inflammation and injury. For example, in a murine heterotopic airway transplant model of bronchiolitis obliterans, *Mmp-8*$^{-/-}$, *Mmp-9*$^{-/-}$, and *Timp-1*$^{-/-}$ mice are all protected from airway luminal collagen deposition and obliteration compared with WT mice (62–64). Similarly, when sensitized and challenged with ovalbumin, *Mmp-8*$^{-/-}$, *Mmp-9*$^{-/-}$ and *Timp-1*$^{-/-}$ mice all have greater allergic airway inflammation than WT mice (18,23,65). *Mmp-8*$^{-/-}$, *Mmp-9*$^{-/-}$, and *Timp-1*$^{-/-}$ mice are also all protected from developing atherosclerosis when crossed with Apo E-deficient mice and fed a cholesterol-rich diet (66–68). These results are consistent with *Timp-1* deficiency leading to loss of membrane-bound Mmp-8 and Mmp-9 on PMNs and possibly other leukocytes that co-express these proteins.

Conclusions: Pro and active forms MMP-8 and MMP-9 that are expressed on the surface of activated PMNs are likely to be important forms of the proteinases *in vivo* as they have similar catalytic activity and efficiency as the soluble forms of the proteinases, but are resistant to inhibition by TIMPs (25,26). This study identified a novel localization for

TIMP-1 on the surface of activated PMNs and in NETs *in vitro*, and on the surface of peripheral blood PMNs of NHPs that were exposed to CS. Surface-bound TIMP-1 on PMNs serves as a receptor for pro and active forms of MMP-8 and MMP-9 and thereby promotes (rather than inhibits) PMN-mediated pericellular proteolysis. Therefore, surface-bound TIMP-1 on PMNs may contribute to extracellular matrix degradation and tissue injury that occurs in COPD, cystic fibrosis, rheumatoid arthritis, and other diseases characterized by neutrophilic inflammation (49–51). Strategies that effectively hinder the binding of TIMP-1 to the surface of PMNs (or the binding of MMP-8 or -9 to membrane-associated TIMP-1) could reduce tissue destruction occurring in these diseases.

Supplementary Material

Refer to Web version on PubMed Central for supplementary material.

Abbreviations used:

ALI	acute lung injury
CS	cigarette smoke
DQ	dye quenched
ECM	extracellular matrix
fMLP	N-formyl-leucyl-methionyl-phenylalanine
HBSS	Hank’s Balanced Salt Solution
HEPES	4-(2-hydroxyethyl)-1-piperazineethanesulfonic acid
IL	interleukin
LPS	lipopolysaccharide
MMP	matrix metalloproteinase
MPO	myeloperoxidase
NET	neutrophil extracellular trap
NHP	non-human primate
PMSF	phenylmethylsulfonyl fluoride
PAF	1-O-hexadecyl-2-acetyl-sn-glycero-3-phosphorylcholine
TIMP	tissue inhibitor of metalloproteinase
TNF-α	tumor necrosis factor-α

References

1. Hasty KA, Pourmotabbed TF, Goldberg GI, Thompson JP, Spinella DG, Stevens RM, and Mainardi CL. 1990 Human neutrophil collagenase. A distinct gene product with homology to other matrix metalloproteinases. J. Biol. Chem 265: 11421–11424. [PubMed: 2164002]
2. Quintero PA, Knolle MD, Cala LF, Zhuang Y, and Owen CA. 2010 Matrix metalloproteinase-8 inactivates macrophage inflammatory protein-1 alpha to reduce acute lung inflammation and injury in mice. J. Immunol 184: 1575–1588. [PubMed: 20042585]
3. Herman MP, Sukhova GK, Libby P, Gerdes N, Tang N, Horton DB, Kilbride M, Breitbart RE, Chun M, and Schonbeck U. 2001 Expression of neutrophil collagenase (matrix metalloproteinase-8) in human atheroma: a novel collagenolytic pathway suggested by transcriptional profiling. Circulation 104: 1899–1904. [PubMed: 11602491]
4. Prikk K, Maisi P, Pirila E, Sepper R, Salo T, Wahlgren J, and Sorsa T. 2001 In vivo collagenase-2 (MMP-8) expression by human bronchial epithelial cells and monocytes/macrophages in bronchiectasis. J Pathol 194: 232–238. [PubMed: 11400153]
5. Owen CA 2008 Leukocyte cell surface proteinases: regulation of expression, functions, and mechanisms of surface localization. Int. J Biochem. Cell Biol 40: 1246–1272. [PubMed: 18329945]
6. Liu Z, Shipley JM, Vu TH, Zhou X, Diaz LA, Werb Z, and Senior RM. 1998 Gelatinase B-deficient mice are resistant to experimental bullous pemphigoid. J. Exp. Med 188: 475–482. [PubMed: 9687525]
7. Sires UI, Murphy G, Welgus HG, and Senior RM. 1994 Matrilysin is much more efficient than other metalloproteinases in the proteolytic inactivation of alpha 1-antitrypsin. Biochem. Biophys. Res. Commun 204: 613–620. [PubMed: 7980522]
8. Van Den Steen PE, Proost P, Wuyts A, Van Damme J, and Opdenakker G. 2000 Neutrophil gelatinase B potentiates interleukin-8 tenfold by aminoterminal processing, whereas it degrades CTAP-III, PF-4, and GRO-a and leaves RANTES and MCP-2 intact. Blood 96: 2673–2681. [PubMed: 11023497]
9. Schonbeck U, Mach F, and Libby P. 1998 Generation of biologically active IL-1b by matrix metalloproteinases: a novel caspase-1-independent pathway of IL-1b processing. J. Immunol 161: 3340–3346. [PubMed: 9759850]
10. Ito A, Mukaiyama A, Itoh Y, Nagase H, Thogersen IB, Enghlid JJ, Sasaguri Y, and Mori Y. 1996 Degradation of interleukin 1b by matrix metalloproteinases. J. Biol. Chem 271: 14657–14660. [PubMed: 8663297]
11. Van Den Steen PE, Wuyts A, Husson SJ, Proost P, Van Damme J, and Opdenakker G. 2003 Gelatinase B/MMP-9 and neutrophil collagenase/MMP-8 process the chemokines human GCP-2/CXCL6, ENA-78/CXCL5 and mouse GCP-2/LIX and modulate their physiological activities. Eur. J. Biochem 270: 3739–3749. [PubMed: 12950257]
12. Yu Q, and Stamenkovic I. 2000 Cell surface-localized matrix metalloproteinase-9 proteolytically activates TGF-beta and promotes tumor invasion and angiogenesis. Genes Dev 14: 163–176. [PubMed: 10652271]
13. Owen CA, and Campbell EJ. 1999 The cell biology of leukocyte-mediated proteolysis. J. Leukoc. Biol 65: 137–150. [PubMed: 10088596]
14. Pyo R, Lee JK, Shipley JM, Curci JA, Mao D, Ziporin SJ, Ennis TL, Shapiro SD, Senior RM, and Thompson RW. 2000 Targeted gene disruption of matrix metalloproteinase-9 (gelatinase B) suppresses development of experimental abdominal aortic aneurysms. J. Clin. Invest 105: 1641–1649. [PubMed: 10841523]
15. Churg A, Wang R, Wang X, Onnervik PO, Thim K, and Wright JL. 2007 Effect of an MMP-9/MMP-12 inhibitor on smoke-induced emphysema and airway remodelling in guinea pigs. Thorax 62: 706–713. [PubMed: 17311841]
16. Lim DH, Cho JY, Miller M, McElwain K, McElwain S, and Broide DH. 2006 Reduced peribronchial fibrosis in allergen-challenged MMP-9-deficient mice. Am. J Physiol Lung Cell Mol. Physiol 291: L265–L271. [PubMed: 16825657]
17. Cataldo DD, Tournoy KG, Vermaelen K, Munaut C, Foidart JM, Louis R, Noel A, and Pauwels RA. 2002 Matrix metalloproteinase-9 deficiency impairs cellular infiltration and bronchial

hyperresponsiveness during allergen-induced airway inflammation. Am. J Pathol 161: 491–498. [PubMed: 12163374]

18. McMillan SJ, Kearley J, Campbell JD, Zhu XW, Larbi KY, Shipley JM, Senior RM, Nourshargh S, and Lloyd CM. 2004 Matrix metalloproteinase-9 deficiency results in enhanced allergen-induced airway inflammation. J Immunol 172: 2586–2594. [PubMed: 14764732]
19. Corry DB, Kiss A, Song LZ, Song L, Xu J, Lee SH, Werb Z, and Kheradmand F. 2004 Overlapping and independent contributions of MMP2 and MMP9 to lung allergic inflammatory cell egression through decreased CC chemokines. FASEB J 18: 995–997. [PubMed: 15059974]
20. Albaiceta GM, Gutierrez-Fernandez A, Parra D, Astudillo A, Garcia-Prieto E, Taboada F, and Fueyo A. 2008 Lack of matrix metalloproteinase-9 worsens ventilator-induced lung injury. Am J Physiol Lung Cell Mol. Physiol 294: L535–L543. [PubMed: 18223162]
21. Lian X, Qin Y, Hossain SA, Yang L, White A, Xu H, Shipley JM, Li T, Senior RM, Du H, and Yan C. 2005 Overexpression of Stat3C in pulmonary epithelium protects against hyperoxic lung injury. J. Immunol 174: 7250–7256. [PubMed: 15905571]
22. Balbin M, Fueyo A, Tester AM, Pendas AM, Pitiot AS, Astudillo A, Overall CM, Shapiro SD, and Lopez-Otin C. 2003 Loss of collagenase-2 confers increased skin tumor susceptibility to male mice. Nat. Genet 35: 252–257. [PubMed: 14517555]
23. Gueders MM, Balbin M, Rocks N, Foidart JM, Gosset P, Louis R, Shapiro S, Lopez-Otin C, Noel A, and Cataldo DD. 2005 Matrix metalloproteinase-8 deficiency promotes granulocytic allergen-induced airway inflammation. J. Immunol 175: 2589–2597. [PubMed: 16081833]
24. Gaggar A, Jackson PL, Noerager BD, O'Reilly PJ, McQuaid DB, Rowe SM, Clancy JP, and Blalock JE. 2008 A novel proteolytic cascade generates an extracellular matrix-derived chemoattractant in chronic neutrophilic inflammation. J Immunol 180: 5662–5669. [PubMed: 18390751]
25. Owen CA, Hu Z, Lopez-Otin C, and Shapiro SD. 2004 Membrane-bound matrix metalloproteinase-8 on activated polymorphonuclear cells is a potent, tissue inhibitor of metalloproteinase-resistant collagenase and serpinase. J. Immunol 172: 7791–7803. [PubMed: 15187163]
26. Owen CA, Hu Z, Barrick B, and Shapiro SD. 2003 Inducible expression of tissue inhibitor of metalloproteinases-resistant matrix metalloproteinase-9 on the cell surface of neutrophils. Am. J. Resp. Cell Mol. Biol 29: 283–294.
27. Betsuyaku T, Shipley JM, Liu Z, and Senior RM. 1999 Neutrophil emigration in the lungs, peritoneum, and skin does not require gelatinase B. Am. J. Respir. Cell Mol. Biol 20: 1303–1309. [PubMed: 10340950]
28. Atkinson JJ, and Senior RM. 2003 Matrix metalloproteinase-9 in lung remodeling. Am. J. Respir. Cell Mol. Biol 28: 12–24. [PubMed: 12495928]
29. Vu TH, and Werb Z. 1998 Gelatinase B: structure, regulation, and function In Matrix Metalloproteinases Parks WC and Mecham RP, eds. Academic Press, San Diego 115–148.
30. Stefanidakis M, Ruohtula T, Borregaard N, Gahmberg CG, and Koivunen E. 2004 Intracellular and cell surface localization of a complex between alphaMbeta2 integrin and promatrix metalloproteinase-9 progelatinase in neutrophils. J Immunol 172: 7060–7068. [PubMed: 15153528]
31. Stefanidakis M, Bjorklund M, Ihanus E, Gahmberg CG, and Koivunen E. 2003 Identification of a negatively charged peptide motif within the catalytic domain of progelatinases that mediates binding to leukocyte beta 2 integrins. J Biol Chem 278: 34674–34684. [PubMed: 12824186]
32. Craig VJ, Polverino F, Laucho-Contreras ME, Shi Y, Liu Y, Osorio JC, Tesfaigzi Y, Pinto-Plata V, Gochuico BR, Rosas IO, and Owen CA. 2014 Mononuclear phagocytes and airway epithelial cells: novel sources of matrix metalloproteinase-8 (MMP-8) in patients with idiopathic pulmonary fibrosis. PLoS. ONE 9: e97485. [PubMed: 24828408]
33. Price B, Dennison C, Tschesche H, and Elliott E. 2000 Neutrophil tissue inhibitor of matrix metalloproteinases-1 occurs in novel vesicles that do not fuse with the phagosome. J. Biol. Chem 275: 28308–28315. [PubMed: 10869345]

34. Boyum A 1963 Isolation of mononuclear cells and granulocytes from human blood: Isolation of mononuclear cells by one centrifugation and of granulocytes by combining centrifugation and sedimentation at 1 g. Scand. J. Clin. Lab. Invest 21(Suppl. 97): 77–89.
35. Polverino F, Rojas-Quintero J, Wang X, Petersen H, Zhang L, Gai X, Higham A, Zhang D, Gupta K, Rout A, Yambayev I, Pinto-Plata V, Sholl LM, Cunoosamy D, Celli BR, Goldring J, Singh D, Tesfaigzi Y, Wedzicha J, Olsson H, and Owen CA. 2018 A Disintegrin and Metalloproteinase Domain-8: A Novel Protective Proteinase in Chronic Obstructive Pulmonary Disease. Am. J. Respir. Crit Care Med 198: 1254–1267. [PubMed: 29750543]
36. Wang X, Polverino F, Rojas-Quintero J, Zhang D, Sanchez J, Yambayev I, Lindqvist E, Virtala R, Djukanovic R, Davies DE, Wilson S, O'Donnell R, Cunoosamy D, Hazon P, Higham A, Singh D, Olsson H, and Owen CA. 2018 A Disintegrin and A Metalloproteinase-9 (ADAM9): A Novel Proteinase Culprit with Multifarious Contributions to COPD. Am. J. Respir. Crit Care Med doi: 10.1164/rccm.201711-2300OC.
37. Owen CA, Campbell MA, Sannes PL, Boukedes SS, and Campbell EJ. 1995 Cell-surface-bound elastase and cathepsin G on human neutrophils. A novel, non-oxidative mechanism by which neutrophils focus and preserve catalytic activity of serine proteinases. J. Cell Biol 131: 775–789. [PubMed: 7593196]
38. Owen CA, Campbell MA, Boukedes SS, and Campbell EJ. 1995 Inducible binding of cathepsin G to the cell surface of neutrophils: A mechanism for mediating extracellular proteolytic activity of cathepsin G. J. Immunol 155: 5803–5810. [PubMed: 7499869]
39. Campbell EJ, Campbell MA, and Owen CA. 2000 Bioactive proteinase 3 on the cell surface of human neutrophils: quantification, catalytic activity, and susceptibility to inhibition. J. Immunol 165: 3366–3374. [PubMed: 10975855]
40. Carmona-Rivera C, Zhao W, Yalavarthi S, and Kaplan MJ. 2015 Neutrophil extracellular traps induce endothelial dysfunction in systemic lupus erythematosus through the activation of matrix metalloproteinase-2. Ann. Rheum. Dis 74: 1417–1424. [PubMed: 24570026]
41. Polverino F, Doyle-Eisele M, McDonald J, Wilder JA, Royer C, Laucho-Contreras M, Kelly EM, Divo M, Pinto-Plata V, Mauderly J, Celli BR, Tesfaigzi Y, and Owen CA. 2015 A novel nonhuman primate model of cigarette smoke-induced airway disease. Am. J. Pathol 185: 741–755. [PubMed: 25542772]
42. Owen CA, and Campbell EJ. 1996 Proteinases In ARDS: Acute Respiratory Distress in Adults, First ed. Haslett C and Evans T, eds. Chapman & Hall Medical, London 139–165.
43. Campbell EJ, and Owen CA. 2007 The sulfate groups of chondroitin sulfate- and heparan sulfate-containing proteoglycans in neutrophil plasma membranes are novel binding sites for human leukocyte elastase and cathepsin G. J. Biol. Chem 282: 14645–14654. [PubMed: 17384412]
44. Sela-Passwell N, Rosenblum G, Shoham T, and Sagi I. 2010 Structural and functional bases for allosteric control of MMP activities: can it pave the path for selective inhibition? Biochim. Biophys. Acta 1803: 29–38. [PubMed: 19406173]
45. Zawrotniak M, and Rapala-Kozik M. 2013 Neutrophil extracellular traps (NETs) - formation and implications. Acta Biochim. Pol 60: 277–284. [PubMed: 23819131]
46. Ong CW, Elkington PT, Brilha S, Ugarte-Gil C, Tome-Esteban MT, Tezera LB, Pabisiak PJ, Moores RC, Sathyamoorthy T, Patel V, Gilman RH, Porter JC, and Friedland JS. 2015 Neutrophil-Derived MMP-8 Drives AMPK-Dependent Matrix Destruction in Human Pulmonary Tuberculosis. PLoS. Pathog 11: e1004917. [PubMed: 25996154]
47. Betsuyaku T, Nishimura M, Takeyabu K, Tanino M, Venge P, Xu S, and Kawakami Y. 1999 Neutrophil granule proteins in bronchoalveolar lavage fluid from subjects with subclinical emphysema. Am. J. Respir. Crit. Care Med 159: 1985–1991. [PubMed: 10351949]
48. Pinto-Plata V, Casanova C, Mullerova H, de Torres JP, Corado H, Varo N, Cordoba E, Zeineldine S, Paz H, Baz R, Divo M, Cortopassi F, and Celli BR. 2012 Inflammatory and repair serum biomarker pattern: association to clinical outcomes in COPD. Respir. Res 13: 71. [PubMed: 22906131]
49. Owen CA 2005 Proteinases and oxidants as targets in the treatment of chronic obstructive pulmonary disease. Proc. Am. Thorac. Soc 2: 373–385. [PubMed: 16267366]

50. Rojas-Quintero J, and Owen CA. 2016 Matrix metalloproteinases in cystic fibrosis: Pathophysiologic and therapeutic perspectives, 3 ed. 49–62.
51. Hergrueter AH, Nguyen K, and Owen CA. 2011 Matrix metalloproteinases: all the RAGE in the acute respiratory distress syndrome. Am J Physiol Lung Cell Mol. Physiol 300: L512–L515. [PubMed: 21296893]
52. Wilk CM, Schildberg FA, Lauterbach MA, Cadeddu RP, Frobel J, Westphal V, Tolba RH, Hell SW, Czibere A, Bruns I, and Haas R. 2013 The tissue inhibitor of metalloproteinases-1 improves migration and adhesion of hematopoietic stem and progenitor cells. Exp. Hematol 41: 823–831. [PubMed: 23660069]
53. Ritter LM, Garfield SH, and Thorgeirsson UP. 1999 Tissue inhibitor of metalloproteinases-1 (TIMP-1) binds to the cell surface and translocates to the nucleus of human MCF-7 breast carcinoma cells. Biochem. Biophys. Res. Commun 257: 494–499. [PubMed: 10198240]
54. Parks WC, Lopez-Boado YS, and Wilson CL. 2001 Matrilysin in epithelial repair and defense. Chest 120: 36S–41S. [PubMed: 11451908]
55. Koppisetti RK, Fulcher YG, Jurkevich A, Prior SH, Xu J, Lenoir M, Overduin M, and Van Doren SR. 2014 Ambidextrous binding of cell and membrane bilayers by soluble matrix metalloproteinase-12. Nat. Commun 5: 5552. [PubMed: 25412686]
56. Prior SH, Fulcher YG, Koppisetti RK, Jurkevich A, and Van Doren SR. 2015 Charge-Triggered Membrane Insertion of Matrix Metalloproteinase-7, Supporter of Innate Immunity and Tumors. Structure 23: 2099–2110. [PubMed: 26439767]
57. Butler GS, Butler MJ, Atkinson SJ, Will H, Tamura T, van Westrum SS, Crabbe T, Clements J, D'Ortho M-P, and Murphy G. 1998 The TIMP2 membrane type 1 metalloproteinase "receptor" regulates the concentration and efficient activation of progelatinase A. J. Biol. Chem 273: 871–880. [PubMed: 9422744]
58. Butler GS, Will H, Atkinson SJ, and Murphy G. 1997 Membrane-type-2 matrix metalloproteinase can initiate the processing of progelatinase A and is regulated by the tissue inhibitors of metalloproteinases. Eur. J. Biochem 244: 653–657. [PubMed: 9119036]
59. Jung KK, Liu XW, Chirco R, Fridman R, and Kim HR. 2006 Identification of CD63 as a tissue inhibitor of metalloproteinase-1 interacting cell surface protein. EMBO J 25: 3934–3942. [PubMed: 16917503]
60. Zhang XZ, Pare PD, and Sandford AJ. 2007 PMN degranulation in relation to CD63 expression and genetic polymorphisms in healthy individuals and COPD patients. Int. J. Mol. Med 19: 817–822. [PubMed: 17390088]
61. English WR, Velasco G, Stracke JO, Knauper V, and Murphy G. 2001 Catalytic activities of membrane-type 6 matrix metalloproteinase (MMP25). FEBS Lett 491: 137–142. [PubMed: 11226436]
62. Khatwa UA, Kleibrink BE, Shapiro SD, and Subramaniam M. 2010 MMP-8 promotes polymorphonuclear cell migration through collagen barriers in obliterative bronchiolitis. J. Leukoc. Biol 87: 69–77. [PubMed: 19801498]
63. Chen P, Farivar AS, Mulligan MS, and Madtes DK. 2006 Tissue inhibitor of metalloproteinase-1 deficiency abrogates obliterative airway disease after heterotopic tracheal transplantation. Am. J. Respir. Cell Mol. Biol 34: 464–472. [PubMed: 16388023]
64. Fernandez FG, Campbell LG, Liu W, Shipley JM, Itohara S, Patterson GA, Senior RM, Mohanakumar T, and Jaramillo A. 2005 Inhibition of obliterative airway disease development in murine tracheal allografts by matrix metalloproteinase-9 deficiency. Am. J. Transplant 5: 671–683. [PubMed: 15760390]
65. Sands MF, Ohtake PJ, Mahajan SD, Takyar SS, Aalinkeel R, Fang YV, Blume JW, Mullan BA, Sykes DE, Lachina S, Knight PR, and Schwartz SA. 2009 Tissue inhibitor of metalloproteinase-1 modulates allergic lung inflammation in murine asthma. Clin. Immunol 130: 186–198. [PubMed: 18955015]
66. Laxton RC, Hu Y, Duchene J, Zhang F, Zhang Z, Leung KY, Xiao Q, Scotland RS, Hodgkinson CP, Smith K, Willeit J, Lopez-Otin C, Simpson IA, Kiechl S, Ahluwalia A, Xu Q, and Ye S. 2009 A role of matrix metalloproteinase-8 in atherosclerosis. Circ. Res 105: 921–929. [PubMed: 19745165]

67. Silence J, Collen D, and Lijnen HR. 2002 Reduced atherosclerotic plaque but enhanced aneurysm formation in mice with inactivation of the tissue inhibitor of metalloproteinase-1 (TIMP-1) gene. Circ. Res 90: 897–903. [PubMed: 11988491]

68. Luttun A, Lutgens E, Manderveld A, Maris K, Collen D, Carmeliet P, and Moons L. 2004 Loss of matrix metalloproteinase-9 or matrix metalloproteinase-12 protects apolipoprotein E-deficient mice against atherosclerotic media destruction but differentially affects plaque growth. Circulation 109: 1408–1414. [PubMed: 14993123]

69. Nakajima T, Tesfaigzi Y, Wilder J, Doyle-Eisele M, McDonald J, Celli BR, and Owen CA. 2012 Matrix metalloproteinase-9 (MMP9) on the surface of blood PMNs is a novel and sensitive biomarker of cigarette smoke-induced inflammation in non human primates (NHPs), 185 ed. A1307-https://www.atsjournals.org/doi/abs/10.1164/ajrccm-conference.2012.185.1_MeetingAbstracts.A1307.

Key points:

1. TIMP-1 is rapidly expressed on PMN surfaces when PMNs are activated.
2. Surface-bound TIMP-1 serves as the receptor for MMP-8 and -9 on PMNs.
3. Surface-bound TIMP-1 promotes (rather than inhibits) PMN pericellular proteolysis.

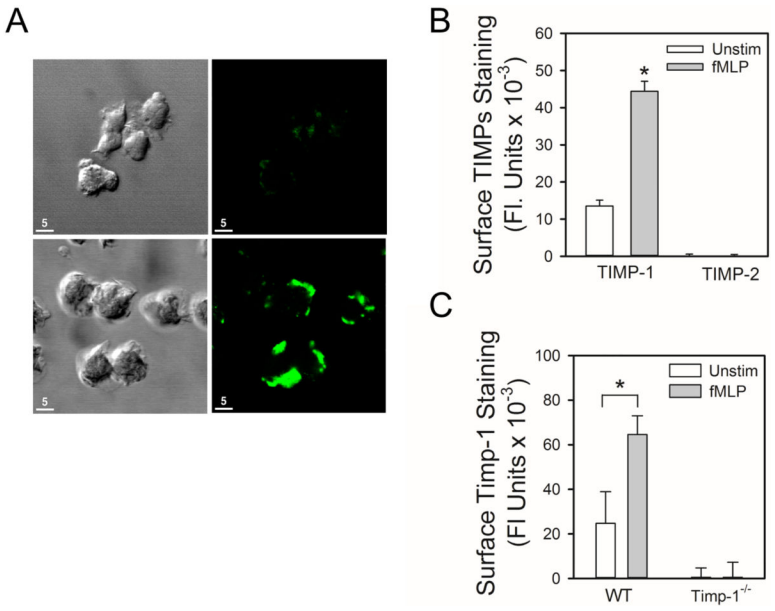

Figure 1: TIMP-1 is expressed in an inducible manner on the surface of activated human and murine PMNs:

In **A**, human PMNs were activated 30 min at 37°C for with 10^{-8} M fMLP and then immunostained with non-immune rabbit IgG (top panel) or rabbit anti-TIMP-1 IgG (bottom panel) followed by goat anti-rabbit $F(ab)_2$-conjugated to Alexa 488. Cells were examined using a Normarski objective (left panels) or confocal microscopy (right panels). The white bars are 5 microns in length. In **B**, human PMNs were incubated 30 min at 37°C with or without 10^{-8} M fMLP and then immunostained with rabbit anti-TIMP-1 IgG, rabbit anti-TIMP-2 IgG, or non-immune rabbit IgG followed by goat anti-rabbit $F(ab)_2$-conjugated to Alexa 488. Images of immunostained cells were captured and analyzed using MetaMorph software. Data are mean + SEM (n = 150–200 cells/group). Data were analyzed using a One-Way ANOVA followed by pair-wise testing with two-tailed Student's t-tests. Asterisk indicates $P < 0.001$ when compared to unstimulated cells stained for surface TIMP-1. In **C**, PMNs isolated from WT or *Timp-1*$^{-/-}$ mice were incubated at 37°C for 30 min with or without 10^{-6} M fMLP, and then immunostained with Alexa 488 for surface Timp-1. Data are mean + SEM; n = 150–200 cells/group. Data were analyzed using a One-Way ANOVA followed by pair-wise testing with two-tailed Student's t-tests. Asterisk indicates $P < 0.001$ compared with unstimulated PMNs. The data shown are representative of at least 3 independent experiments.

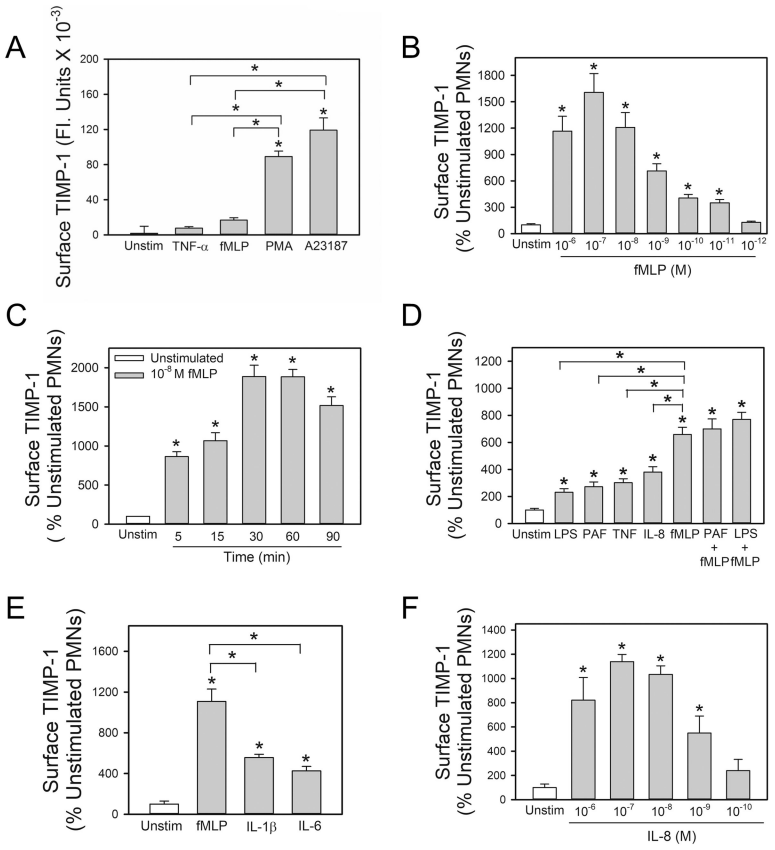

Figure 2: Degranulating agonists rapidly up-regulate surface TIMP-1 levels on human PMNs: Human PMNs were incubated for 30 min at 37°C with (grey bars) or without (open bar) 100 U/ml TNF-α, 10^{-7} M fMLP, 300 nM phorbol myristate acetate (PMA) or 5 μM calcium ionophore (A23187) in **A**, or varying concentrations of fMLP in **B**, or 10^{-7} M fMLP for 1–90 min in **C**. In **D**, human PMNs were incubated for 30 min at 37°C without (open bar) or with (grey bars) LPS (100 ng/ml), PAF (10^{-7} M), TNF-α (100 U/ml), IL-8 (10^{-7} M) and fMLP (10^{-7} M) alone, or PMN were primed for 15 min at 37°C with and without the same concentrations of LPS or PAF and then activated for 30 min with 10^{-7} M fMLP. In **E**, human PMNs were incubated for 30 min at 37°C without or with 10^{-7} M fMLP, 10^{-7} M IL-1β, or 10^{-7} M IL-6, or varying concentrations of IL-8 in **F**. In **A-F**, cells were then fixed and immunostained for surface-bound TIMP-1 and surface TIMP-1 levels were quantified using image analysis software as described in Methods. Data are mean + SEM; n = 150–200 cells per group. In **A-F**, data were analyzed using a One-Way ANOVA followed by pair-wise testing with two-tailed Student's t-tests. Asterisk indicates $P < 0.001$ compared with unstimulated cells or the group indicated. The results shown are representative of at least 3 independent experiments.

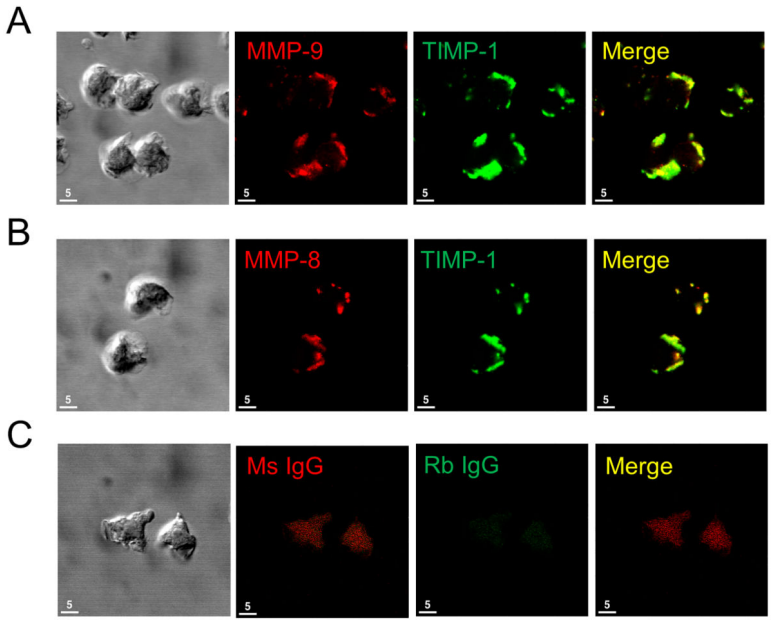

Figure 3: TIMP-1 is co-localized with MMP-8 and MMP-9 on the surface of activated human PMNs:

Human PMNs were activated at 37°C with PAF at 10^{-7} M for 15 min followed by fMLP at 10^{-7} M for 30 min. Cells were double immunostained with Alexa 546 and murine anti-MMP-9 IgG (**A**, second panel), or murine anti-human MMP-8 IgG (**B**, second panel) or non-immune murine (Ms) IgG (**C**, second panel) and with Alexa 488 and rabbit anti-TIMP-1 IgG (**A** and **B** third panels) or non-immune rabbit (Rb) IgG (**C**, third panel). The anti-MMP-8 and anti-MMP-9 IgGs used recognize both pro and active forms of these MMPs. Cells were examined using a Normarski objective (**A-C**, left panels) and co-localization of MMPs and TIMP-1 on the surface of the activated PMNs was assessed by confocal microscopy (see merged images in the right panels for **A-C**). The white bars are 5 microns in length. Note the strong co-localization of TIMP-1 with both MMP-8 and MMP-9 on the surface of activated PMNs. The results shown are representative of at least 3 different PMN preparations.

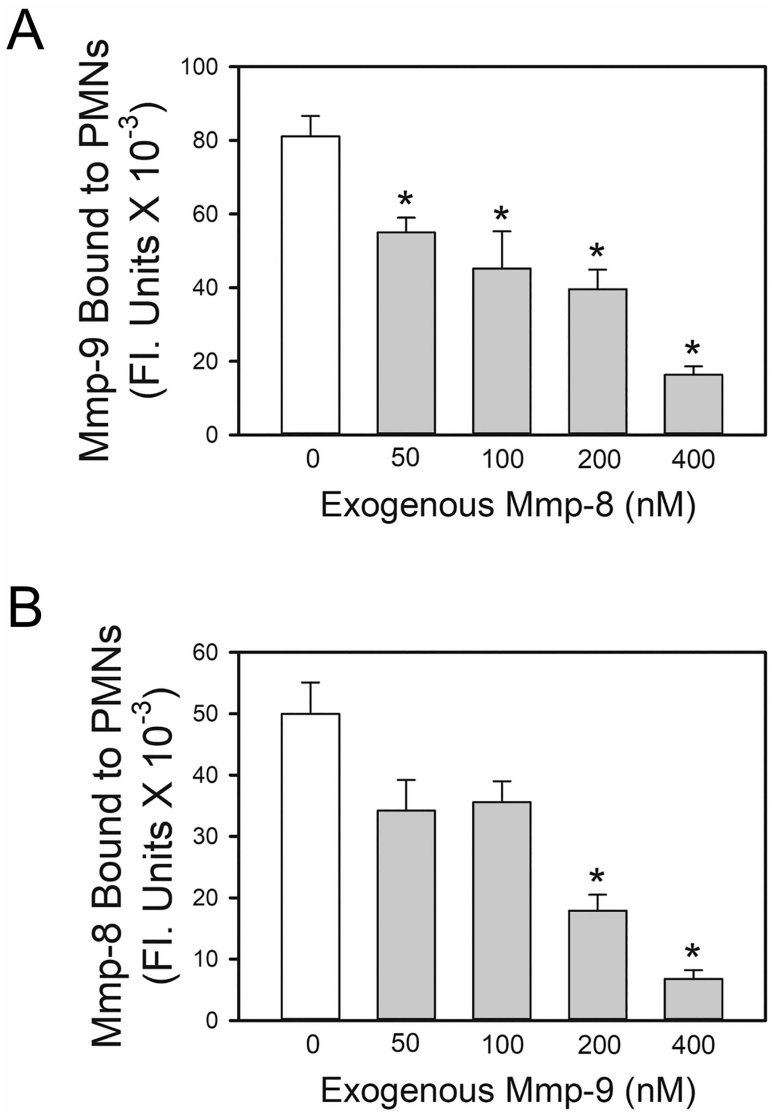

Figure 4: ProMMP-8 and proMMP-9 share binding sites on the surface of PMNs:

In **A** and **B**, PMNs from *Mmp-8*$^{-/-}$ *x Mmp-9*$^{-/-}$ mice were activated for 15 min at 37°C with 10^{-6} M PAF followed by 10^{-6} M fMLP to induce surface expression of Timp-1. In **A**, the activated PMNs were then pre-incubated for 45 min at 4°C with or without exogenous full length murine proMmp-8 (50–400 nM). Cells were then incubated for an additional 60 min at 4°C with 100 nM exogenous murine proMMP-9. Cells were then washed and immunostained with rabbit anti-murine Mmp-9 IgG, or non-immune rabbit IgG followed by goat anti-rabbit $F(ab)_2$-conjugated to Alexa 488 to detect bound pro and active Mmp-9. In **B**, the PAF- and fMLP- activated and PMNs were pre-incubated for 45 min at 4°C with or without exogenous full length murine proMmp-9 (50–400 nM). Cells were then incubated for an additional 60 min at 4°C with 100 nM exogenous full length murine proMMP-8. Cells were then immunostained with rabbit anti-murine Mmp-8 IgG, or non-immune rabbit IgG followed by goat anti-rabbit $F(ab)_2$-conjugated to Alexa 488 to detect bound pro and active Mmp-8. In **A** and **B**, images of immunostained cells were captured and surface-bound pro

and active Mmp-9 (in **A**) or pro and active Mmp-8 (in **B**) were quantified using MetaMorph software. Data are mean + SEM (n = 150–200 cells/group). Data were analyzed using a One-Way ANOVA followed by pair-wise testing with two-tailed Student's t-tests. Asterisk indicates $P < 0.001$ when compared with PMNs incubated in the absence of exogenous Mmp. The results shown are representative of at least 3 independent experiments.

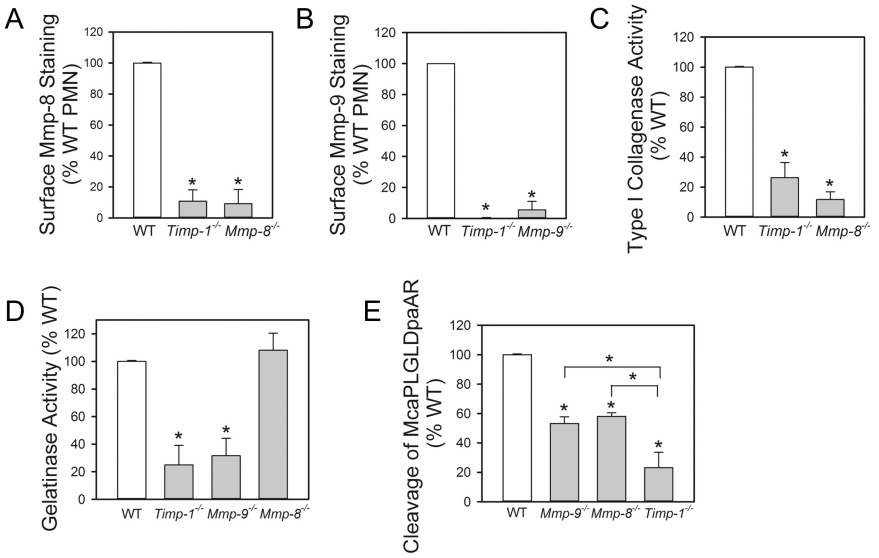

Figure 5: Immunoreactive and active levels of Mmp-8 and Mmp-9 are markedly reduced on the surface of *Timp-1*$^{-/-}$ PMNs:

In **A** and **B**, PMNs from WT, *Timp-1*$^{-/-}$, *Mmp-8*$^{-/-}$, and *Mmp-9*$^{-/-}$ mice were activated for 15 min at 37°C with 10^{-6} M PAF followed by 10^{-6} M fMLP. The cells were then fixed and immunostained for surface-bound Mmp-8 (in **A**) or surface-bound Mmp-9 (in **B**) using antibodies that detect both pro and active forms of these Mmps. Surface levels of Mmp-8 or Mmp-9 were quantified as described in Methods and expressed as a percentage of the amount of Mmp-8 or Mmp-9 respectively, that were expressed on the surface of activated WT PMNs. Data are mean + SEM from 3–4 separate experiments. Data were analyzed using a One-Way ANOVA followed by pair-wise testing with two-tailed Student's t-tests. Asterisk indicates $P < 0.01$ compared with WT PMNs. In **C**-**E**, PMNs from WT, *Timp-1*$^{-/-}$, and *Mmp-8*$^{-/-}$ and or *Mmp-9*$^{-/-}$ mice were activated and fixed as described in **A**. Equal numbers of cells from each genotype were pre-incubated for 1 h at 37°C in triplicate with and without 1–10-phenanthroline (a non-selective MMP inhibitor). Cells were then incubated at 37°C with: 1) type I-collagen conjugated to quenched FITC for 18 h (in **C**); 2) gelatin conjugated to quenched FITC for 6 h (in **D**); or 3) McaPLGLDpaAR (a quenched fluorogenic peptide substrate which is cleaved by both Mmp-8 and Mmp-9) for 3 h (in **E**). Mmp-mediated cleavage of each substrate was quantified in cell-free supernatant samples by fluorimetry as the 1,10-phenanthroline-inhibitable cleavage of the substrate, as described in Methods. The data are expressed as mean + SEM % cleavage of the substrate by WT cells from 4–5 separate experiments. Data were analyzed using a One-Way ANOVA followed by pair-wise testing with two-tailed Student's t-tests. Asterisk indicates $P < 0.01$ compared with WT PMNs or the group indicated.

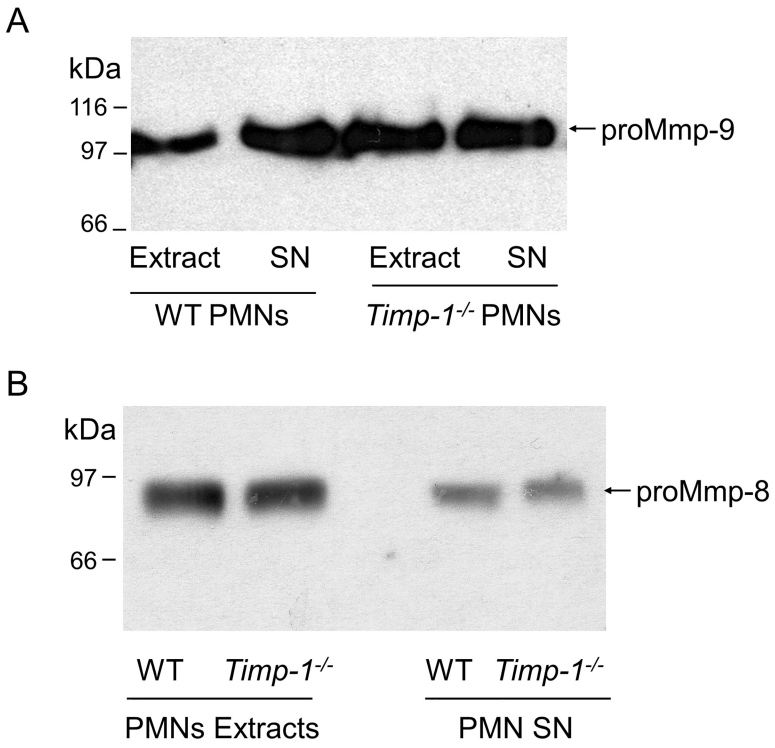

Figure 6: WT and *Timp-1*$^{-/-}$ PMN contain similar amounts of Mmp-8 and Mmp-9 and similar quantities of Mmp-8 and Mmp-9 are released from degranulating WT and *Timp-1*$^{-/-}$ PMNs:

Extracts of freshly-isolated unstimulated PMNs from WT and *Timp-1*$^{-/-}$ mice and cell-free supernatant fluids from WT and *Timp-1*$^{-/-}$ PMN that had been activated with 10^{-6} M fMLP for 30 min were immuno-blotted for Mmp-9 (**A**) or Mmp-8 (**B**). The arrows indicate the proMMP-9 and proMmp-8 forms of the Mmps. Note that extracts of unstimulated WT and *Timp-1*$^{-/-}$ PMNs contain similar amounts of proMmp-9 and proMmp-8 (M_r = 100 kDa for Mmp-9 and 85 kDa for Mmp-8). In addition, when activated with fMLP, *Timp-1*$^{-/-}$ PMNs freely release similar amounts of Mmp-8 and Mmp-9 exclusively as the latent proMmp forms.

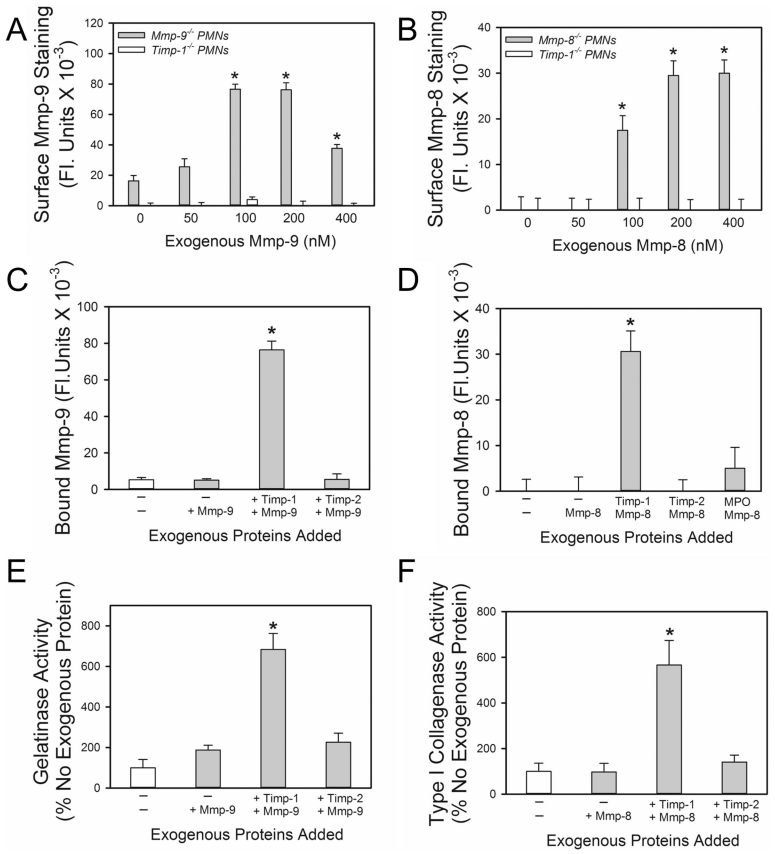

Figure 7: Exogenous Timp-1 reconstitutes the binding of exogenous proMmp-9 and proMmp-8 to *Timp-1*$^{-/-}$ PMNs:

In **A**, PAF- and fMLP-activated PMNs from *Mmp-9*$^{-/-}$ and *Timp-1*$^{-/-}$ mice were incubated with or without 50–400 nM exogenous murine proMmp-9, and then immunostained with rabbit anti-Mmp-9 IgG, or non-immune rabbit IgG followed by goat anti-rabbit F(ab)$_2$-conjugated to Alexa 488. In **B**, PAF- and fMLP-activated PMNs from *Mmp-8*$^{-/-}$ and *Timp-1*$^{-/-}$ mice were incubated with or without 50–400 nM exogenous murine proMmp-8, and then immunostained with rabbit anti-Mmp-8 IgG, or non-immune rabbit IgG followed by goat- anti-rabbit F(ab)$_2$-conjugated to Alexa 488. In **A-B**, the antibodies used detect both the pro and active forms of the Mmps. Data are mean + SEM; n = 150–200 cells per group. Data were analyzed using a One-Way ANOVA followed by pair-wise testing with two-tailed Student's t-tests. Asterisk indicates $P < 0.001$ compared with cells incubated without exogenous murine proMmp-9 or proMmp-8. In **C**, *Timp-1*$^{-/-}$ PMNs were incubated at 4°C with: 1) no exogenous proteins for 2 h; 2) no exogenous proteins for 1 h and then 200 nM proMmp-9 for 1 h; 3) 200 nM Timp-1 for 1 h and then with proMmp-9 for 1 h; 4) 200 nM Timp-2 for 1 h, and then with proMmp-9 for 1 h. Unbound proteins were removed after each incubation step by washing PMN twice in buffer. Non-permeabilized PMNs were then immunostained with Alexa 488 for surface-bound pro and active Mmp-9. Data are mean + SEM; n = 150–200 cells per group. Data were analyzed using a One-Way ANOVA followed by pair-wise testing with two-tailed Student's t-tests. Asterisk indicates $P < 0.001$ compared with all other groups. In **D**, *Timp-1*$^{-/-}$ PMN were incubated at 4°C with: 1) no exogenous proteins for 2 h; 2) no exogenous proteins for 1 h and then 200 nM proMmp-8 for 1 h; 3)

200 nM Timp-1 for 1 h and then proMmp-8 for 1 h; 4) 200 nM Timp-2 for 1 h and then proMmp-8 for 1 h; 5) 200 nM myeloperoxidase for 1 h and then 200 nM proMmp-8 for 1 h. Unbound proteins were removed after each incubation step by washing PMN twice in PBS. Non-permeabilized PMNs were then immunostained with Alexa 488 for surface-bound pro and active Mmp-8. Data are mean + SEM; n = 150–200 cells per group. Data were analyzed using a One-Way ANOVA followed by pair-wise testing with two-tailed Student's t-tests. Asterisk indicates $P < 0.001$ compared with all other groups. In **A-D**, the results shown are representative of at least 3 independent experiments. In **E-F**, equal numbers of PAF- and fMLP-activated PMNs from *Timp-1*$^{-/-}$ mice were incubated at 4°C with: 1) no exogenous proteins for 2 h; 2) no exogenous proteins for 1 h and 200 nM proMmp-9 or proMmp-8 alone for 1 h; 3) 200 nM Timp-1 for 1 h and then 200 nM proMmp-9 or proMmp-8 for 1 h; 4) 200 nM Timp-2 for 1 h and then 200 nM proMmp-9 or proMmp-8 for 1 h; The cells were fixed and then incubated at 37°C with: 1) gelatin conjugated to quenched FITC for 18 h (in **E**); or 2) type-I collagen conjugated to quenched FITC for 18 h (in **F**). In **E-F**, Mmp-mediated cleavage of each substrate in the presence of amino-phenyl mercuric acetate was quantified in cell-free supernatant samples using fluorimetry, as described in Methods. The data are expressed as mean + SEM % cleavage of the substrate in cells incubated without exogenous proteins; n=4–5 separate experiments. Data were analyzed using a Kruskal-Wallis One-Way ANOVA followed by pair-wise testing with Mann-Whitney U tests. Asterisks indicate $P < 0.05$ compared with all other groups.

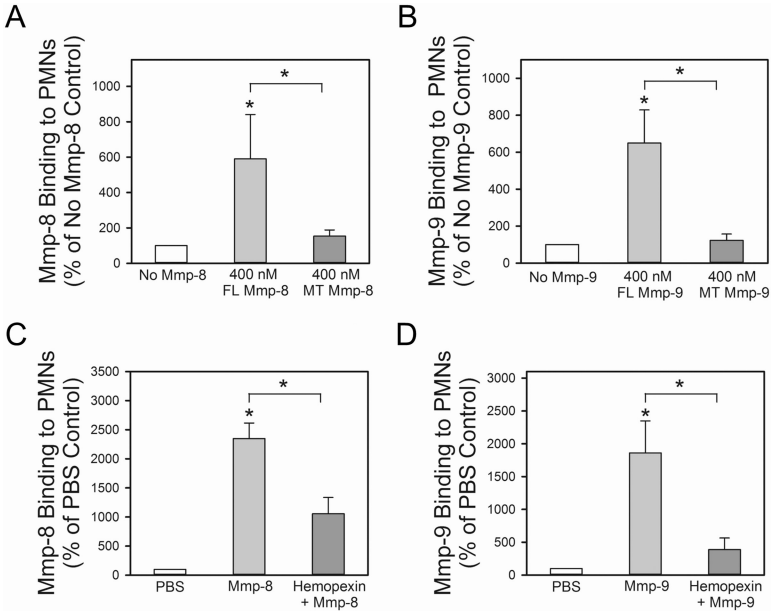

Figure 8: The COOH-terminal hemopexin domain of both proMmp-8 and proMmp-9 is required for the binding of these proteinases to the surface of activated PMNs:

In **A**, PAF- and fMLP-activated *Mmp-8*$^{-/-}$ *x Mmp-9*$^{-/-}$ PMNs were incubated for 2 h at 4°C with or without 400 nM full length proMmp-8 protein (FL Mmp8) or 400 nM mutant proMmp-8 protein lacking the COOH-terminal hemopexin domain (MT Mmp-8). Bound Mmp-8 was detected by immunostaining cells with Alexa 488 using an antibody raised to the hinge region of Mmp-8 (which is present in both the FL and MT forms of Mmp-8). In **B**, PAF- and fMLP-activated *Mmp-8*$^{-/-}$ *x Mmp9*$^{-/-}$ PMNs were incubated for 2 h at 4°C with or without 400 nM full length Mmp-9 (FL Mmp9) or 400 nM mutant Mmp-9 lacking the COOH-terminal hemopexin domain (MT Mmp9). Bound Mmp-9 was detected by immunostaining cells with Alexa 488 using an antibody raised to the hinge region of Mmp-9 (which is present in both the FL and MT forms of Mmp-8 and Mmp-9). In **A**-**B**, Data are mean + SEM; n = 3 separate experiments each analyzing 300 cells/group). Data were analyzed using a One-Way ANOVA followed by pair-wise testing with two-tailed Student's t-tests. Asterisk indicates $P < 0.05$ compared with the no exogenous Mmp group or the group indicated. In **C**-**D**, PAF- and fMLP-activated *Mmp-8*$^{-/-}$ *x Mmp9*$^{-/-}$ PMNs were incubated at 4°C for 60 min with or without 500 nM soluble murine hemopexin protein. Cells were then incubated at 4°C for 60 min with or without 400 nM exogenous proMmp-8 or 400 nM exogenous proMmp-9. Mmp-8 and Mmp-9 that bound to cells was detected by immunostaining the cells with Alexa-488 for Mmp-8 (**C**) or Mmp-9 (**D**), as described above. Data are mean + SEM; n = 3 separate experiments each analyzing 300 cells/group. Data were analyzed using a One-Way ANOVA followed by pair-wise testing with two-tailed Student's t-tests. Asterisk indicates $P < 0.05$ compared with the group incubated without exogenous proteins or the group indicated.

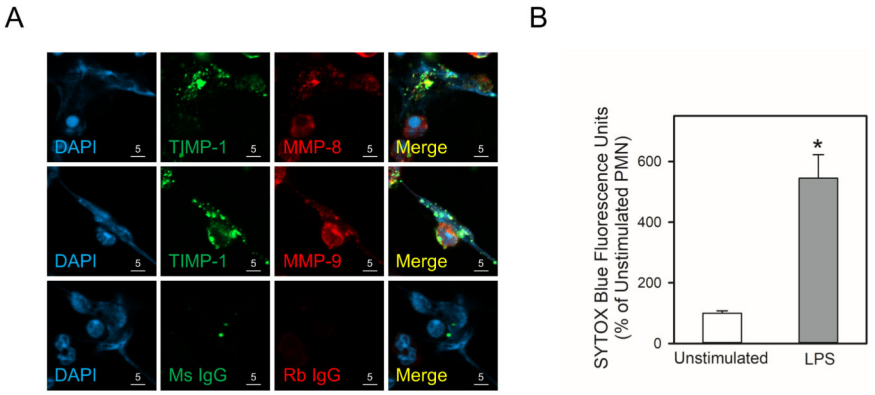

Figure 9: TIMP-1 is co-localized with MMP-8 and MMP-9 in PMN extracellular traps (NETs): In **A** and **B**, human PMNs were incubated with 1 μg/mL LPS for 4 h at 37°C to induce NET formation, or without LPS as a control. In **A**, the cells were fixed and then double immunostained with a green fluorophore for TIMP-1 (second panels) and a red fluorophore for MMP-8 or MMP-9 (third panels). Nuclei were counterstained blue with 4',6-diamidino-2-phenylindole (DAPI). Co-localization of TIMP-1 and MMPs in PMN-associated NETs was assessed by confocal microscopy (see merged images in the fourth panels). The results shown are representative of 4 different PMN preparations. In **B**, NET induction by LPS was quantified by staining the samples for extracellular DNA with SYTOX™ Blue Nucleic Acid Stain, and quantifying the staining as described in Methods. Data are mean + SEM; n = 4 experiments. Data were analyzed using the Mann-Whitney U tests. Asterisk indicates $P < 0.05$ compared with unstimulated cells.

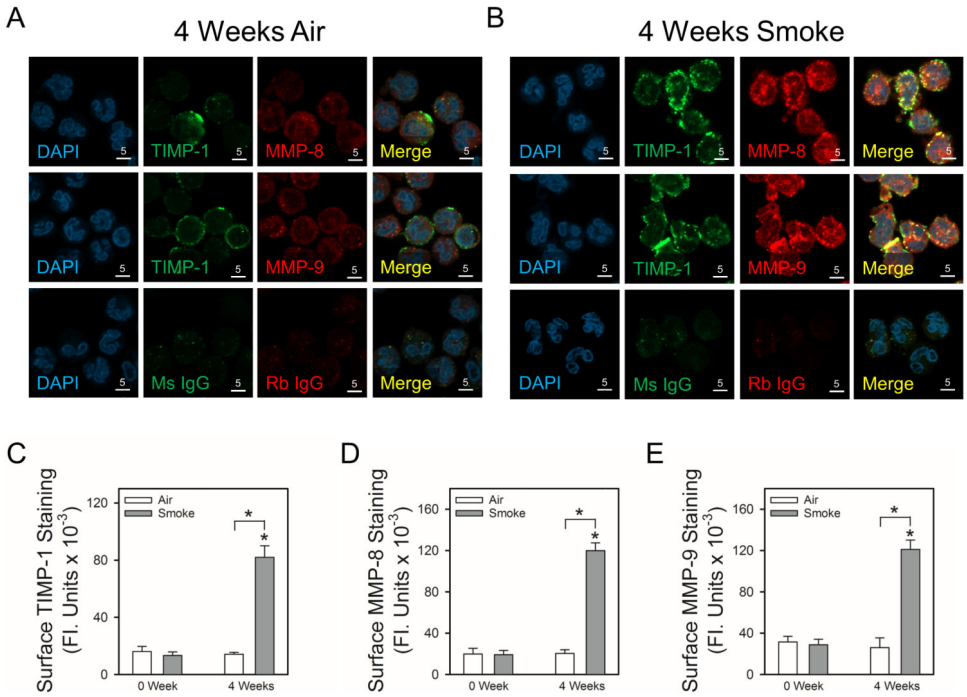

Figure 10: Exposure of non-human primate (NHP) to cigarette smoke increases co-localized expression of TIMP-1 with MMP-8 and MMP-9 on the surface of peripheral blood PMNs: NHPs were exposed to air (n = 4; white bars) or smoke (n = 6; gray bars) for 4 weeks, and PMNs were isolated from peripheral blood samples from each animal both at baseline and after 4 weeks of air or CS exposure. Cells were double immunostained with Alexa 488 and murine anti-TIMP-1 IgG or non-immune murine (Ms) IgG (**A** and **B** second panels) and with Alexa 546 and rabbit anti-MMP-8 IgG or rabbit anti-MMP-9 IgG (**A** and **B** third panels). Nuclei in the cells were counterstained blue using 4',6-diamidino-2-phenylindole (DAPI, **A** and **B** first panels). Co-localization of TIMP-1 and MMPs on the surface of PMNs was assessed using confocal microscopy (see merged images in the fourth panels in **A** and **B**). The white bars are 5 microns in length. In **C**-**E**, surface TIMP-1 or MMPs levels were quantified using image analysis software, as described in Methods. Data are mean + SEM; n = 4 air-exposed NHPs and n = 6 smoke-exposed NHPs (200–500 cells were analyzed per animal). In **C**-**E**, data were analyzed using a One-Way ANOVA followed by pair-wise testing with two-tailed Student's t-tests. Asterisk indicates $P < 0.001$ compared with baseline or the group indicated.

Table I:

Mmp-9 protein levels contained within and released by WT and *Timp-1*$^{-/-}$ PMNs

Condition	Mmp-9 (ng/10^6 cells)	*P* Value*
Unstimulated WT PMN extracts	45.8 (10.9)	
Unstimulated *Timp-1*$^{-/-}$ PMN extracts	76.9 (10.7)	*P* = 0.0764
Supernatant fluids from activated WT PMNs	7.4 (3.2)	
Supernatant fluids from activated *Timp-1*$^{-/-}$ PMNs	10.7 (5.9)	*P* = 0.302

A. Extracts of freshly isolated unstimulated WT and *Timp-1*$^{-/-}$ PMNs were prepared and assayed in duplicate to quantify Mmp-9 levels using an ELISA.

B. WT and *Timp-1*$^{-/-}$ PMNs were incubated at 37°C with or without 10^{-6}M fMLP for 30 min and cell-free supernatants samples harvested and assayed in duplicate to quantify Mmp-9 levels using an ELISA.

C. Data are mean ± SD (n = 5 different cell preparations per condition).

**P* value for comparison with WT samples.

Table II:

Mmp-8 protein levels contained within and released by WT and *Timp-1*$^{-/-}$ PMNs

Condition	Mmp-8 (pg/10^6 cells)	*P* Value*
Unstimulated WT PMN extracts	498.5 (63.1)	
Unstimulated *Timp-1*$^{-/-}$ PMN extracts	473.2 (135.7)	*P* = 0.663
Supernatant fluids from activated WT PMNs	254.1 (51.2)	
Supernatant fluids from activated *Timp-1*$^{-/-}$ PMNs	213.5 (36.4)	*P* = 0.113

A. Extracts of freshly-isolated unstimulated WT and *Timp-1*$^{-/-}$ PMNs were prepared and assayed in duplicate to quantify Mmp-8 levels using an ELISA.

B. WT and *Timp-1*$^{-/-}$ PMNs were incubated at 37°C with or without 10^{-6}M fMLP for 30 min and cell-free supernatants samples harvested and assayed in duplicate to quantify Mmp-8 levels using an ELISA.

C. Data are mean ± SD (n = 7 different cell preparations per condition).

**P* value for comparison with WT samples.